ACS OMEGA

Open Access

This article is licensed under CC-BY 4.0

http://pubs.acs.org/journal/acsodf

Article

Production Optimization and Functional Characterization of Melanin Produced by Halotolerant *Bacillus atrophaeus* Isolated from a Hypersaline Environment

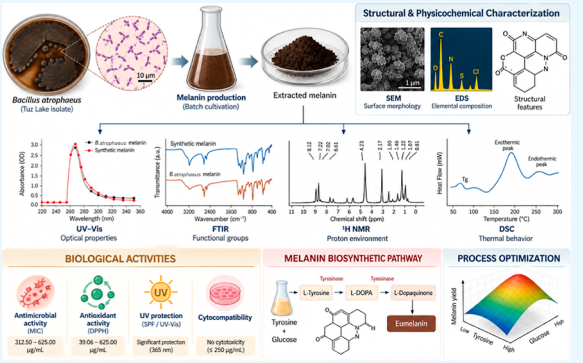
Pervin Soyer,* Semra İlhan, A. Alper Öztürk, and Yağmur Tunali

Cite This: https://doi.org/10.1021/acsomega.6c03470

Read Online

ACCESS | Metrics & More | Article Recommendations

ABSTRACT: Melanin is a naturally occurring dark biopolymer widely distributed in microorganisms, plants, and animals, known for its remarkable physicochemical properties, including ultraviolet (UV) protection and antioxidant activity. In this study, a halotolerant bacterial isolate obtained from the hypersaline environment of Tuz Lake was identified as *Bacillus atrophaeus* and evaluated as a novel source of microbial melanin. The strain was cultivated under batch conditions, and melanin production was optimized using a Box−Behnken experimental design to maximize pigment yield. The extracted melanin was comprehensively characterized by solubility analysis, UV−vis spectroscopy, Fourier-transform infrared (FT-IR) spectroscopy, differential scanning calorimetry (DSC), proton nuclear magnetic resonance (^{1}H NMR) spectroscopy, and scanning electron microscopy coupled with energy-dispersive X-ray spectroscopy (SEM−EDS). Comparative analyses with commercial synthetic melanin revealed similarities in physicochemical, thermal, morphological, and spectroscopic characteristics, supporting the classification of the extracted material as a DOPA-dependent eumelanin-like pigment. Biological activity assays demonstrated antimicrobial activity with minimum inhibitory concentration (MIC) values ranging from 312.50 to 625.00 μg/mL, concentration-dependent antioxidant activity (39.06−625.00 μg/mL) in the DPPH assay, and significant UV-protective effects, while no cytotoxicity was observed up to 250 μg/mL. Biosynthetic pathway analysis, together with the inhibitor response and ^{1}H NMR findings, supported the involvement of a tyrosinase-mediated DOPA pathway in pigment formation with tyrosine and glucose playing important roles in production enhancement. This study identifies halotolerant *Bacillus atrophaeus* as a promising microbial source of a functionally active DOPA-dependent eumelanin-like pigment with potential pharmaceutical, cosmetic, and biotechnological applications.



1. INTRODUCTION

In recent years, pigments derived from natural sources have attracted increasing global interest and have gained significant importance. With growing awareness of the beneficial effects of natural compounds on human health, the demand for pigments produced from natural sources continues to rise. Although a wide variety of natural pigments can be obtained from insects, plants, and animals, microbial pigments stand out due to their ease of production, rapid yield, and the possibility of controlled synthesis under defined conditions. The expanding global market for microbial pigments has further stimulated the development of diverse production strategies and application areas. In particular, halophilic and halotolerant microorganisms produce various pigments as an adaptive response to extreme environmental conditions. Pigment accumulation is generally enhanced under stress conditions such as high salinity, nutrient limitation, and elevated radiation levels, where slower cellular growth is associated with increased pigment production.[1]

Melanin is a complex, amorphous, and heterogeneous biopolymer widely distributed in nature, ranging from microorganisms to humans, and is primarily composed of indolic and phenolic structural units.[2,3] The term "melanin" originates from the Greek word "melanos", meaning dark, and was first introduced into scientific literature in 1840 by the Swedish chemist Berzelius.[2] Melanins represent a diverse group of polymers with broad structural variability and multifunctional biological activities, including antitumor, antiviral, antimicrobial, anti-inflammatory, and radioprotective effects.[4] Owing to these properties, melanins have been widely utilized in various fields such as textiles, dyes, medicine,

Received: March 29, 2026
Revised: October 8, 2026
Accepted: October 13, 2026

ACS Publications

© XXXX The Authors. Published by American Chemical Society

Downloaded from pubs.acs.org/acsodf/article-pdf/doi/10.1021/acsomega.6c03470/6922768l/acsomega.6c03470.pdf by ANADOLU UNIV. Pervin Soyer on 18 November 2026

pharmaceuticals, cosmetics, materials science, food, and coating technologies.

Melanin synthesis begins at very early stages of life in living organisms and plays a crucial role in protection against environmental stress factors.[5] In particular, melanin provides protection against ultraviolet (UV) radiation, extreme temperature fluctuations, and oxidative stress. Therefore, melanin production is considered an evolutionary adaptation mechanism that enables organisms to survive under changing environmental conditions. Melanin is synthesized by a wide range of organisms, including plants, animals, and microorganisms. Notably, melanin derived from microbial sources offers several advantages over that obtained from plants and animals.[2,3] Microorganisms can be cultivated independently of seasonal variations and can produce melanin efficiently under controlled culture conditions. In contrast, the development of environmentally friendly and cost-effective melanin production from eukaryotic sources remains challenging, which has further increased interest in microbial melanins.[6−8] Among melanin-producing microorganisms, bacterial genera such as *Streptomyces*, *Pseudomonas*, *Nocardiopsis*, *Bacillus*, *Klebsiella*, *Rhizobium*, *Vibrio*, and *Thermomicrobium*, as well as fungal genera including *Saccharomyces*, *Cryptococcus*, *Armillaria*, and *Aspergillus*, have been reported as important producers. Melanins derived from these microorganisms are considered a unique class of natural biomaterials with diverse industrial applications.

Melanin pigments are classified based on their chemical structure and monomer composition into eumelanin, pheomelanin, pyomelanin, neuromelanin, and allomelanin.[2] Eumelanin and allomelanin typically impart black or brown coloration, whereas pheomelanin contributes to yellow, red, or light brown pigmentation.[8] Additionally, melanins can be categorized according to their biosynthetic pathways into DOPA-melanin and DHN-melanin. These types are predominantly produced by bacteria and fungi. The primary similarity among these systems lies in the formation of polymeric structures through covalent bonding of monomer units; however, differences in enzyme systems and precursor molecules contribute to the structural heterogeneity of melanins.

In the DOPA-melanin biosynthetic pathway, the amino acid tyrosine is oxidized by the enzyme tyrosinase to form L-DOPA (3,4-dihydroxyphenylalanine). Subsequent oxidation of L-DOPA via dopaquinone leads to the formation of indole derivatives such as 5,6-dihydroxyindole and 5,6-dihydroxyindole-2-carboxylic acid, which polymerize to form melanin. Eumelanin and pheomelanin are synthesized via this pathway. These pigments exhibit essential biological functions, including absorption of UV radiation, neutralization of free radicals, and strong antioxidant activity.[9]

Among melanin-producing microorganisms, bacteria have gained particular attention due to their rapid growth rates, genetic adaptability, and resilience to harsh environmental conditions. In particular, species belonging to the genus *Bacillus* are of significant biotechnological interest owing to their robust physiology, spore-forming capability, tolerance to environmental stress, and suitability for large-scale fermentation processes. Nevertheless, melanin production in bacteria is highly strain-dependent, and many *Bacillus* species remain insufficiently explored in terms of their melanogenic potential. *Bacillus atrophaeus* is a Gram-positive, spore-forming bacterium that has been extensively studied as a model organism for spore resistance, sterilization validation, and environmental monitoring.[10] Despite its well-established industrial and microbiological relevance, the capacity of *B. atrophaeus* to produce melanin has received limited attention, and studies describing melanin biosynthesis in this species are scarce. Furthermore, comprehensive investigations focusing on the structural and biological properties of melanin derived from *B. atrophaeus* isolates are largely lacking. This gap is particularly significant in light of the increasing demand for novel microbial melanin sources with distinct structural and functional characteristics. Studies on halotolerant *Bacillus atrophaeus* strains isolated from hypersaline environments are still few, despite the fact that microbial melanin synthesis has been thoroughly studied in a number of bacterial and fungal species. Specifically, the optimization of melanin production and the thorough physicochemical and biological characterization of melanins produced by halotolerant strains of *B. atrophaeus* are lacking. Investigating such isolates could lead to the discovery of melanins with improved biological properties and industrial applicability because microorganisms adapted to extreme saline environments may synthesize structurally and functionally distinct melanins to survive under harsh environmental conditions.

In this study, a melanin-like pigment produced by a halotolerant *Bacillus atrophaeus* isolate from a hypersaline environment was investigated in terms of its physicochemical, structural, and biological properties. In addition, the melanin production process was optimized using an experimental design approach to enhance pigment yield under controlled conditions. The obtained pigment was characterized using complementary spectroscopic, thermal, morphological, and elemental techniques, and its biosynthetic pathway was evaluated using pathway-specific inhibitors. The findings of this study are expected to contribute to the expanding knowledge of bacterial melanin and to support its potential applications in microbiology, biotechnology, food, and health-related fields. The combined analyses were used to assess whether the pigment exhibited characteristics consistent with a DOPA-dependent eumelanin-like material.

2. MATERIALS AND METHODS

2.1. Chemicals

All chemicals and culture media used in this study were of analytical or microbiological grade. Peptone, yeast extract, beef extract, agar, D-(+)-glucose, L-tyrosine, copper sulfate ($CuSO_4$), sodium chloride (NaCl), Mueller Hinton agar/broth (MHA/MHB), phosphate-buffered saline (PBS), methanol, ethanol, acetone, chloroform, ethyl acetate, dimethyl sulfoxide (DMSO), and acetic acid were purchased from Merck (Germany). Nutrient agar (NA) was obtained from Biolife (Italy), and Sabouraud dextrose agar (SDA) was obtained from BIOMARK (India). Dulbecco's Modified Eagle Medium (DMEM), penicillin/streptomycin, and fetal bovine serum (FBS) used for cell culture studies were obtained from Gibco (USA) and Capricorn Scientific (USA). DPPH, MTT, erythromycin, fluconazole, kojic acid, tricyclazole, phthalide, and synthetic melanin were purchased from Sigma-Aldrich (USA).

Synthetic melanin (Sigma-Aldrich, St. Louis, MO, USA; product no. M8631; CAS no. 8049-97-6) was used as the reference material in the comparative analyses. According to the manufacturer, the product is prepared by the oxidation of tyrosine with hydrogen peroxide and is classified as a synthetic eumelanin-type pigment. The synthetic melanin was dissolved in 0.1 M sodium hydroxide (NaOH), diluted to the required concentrations, and tested under the same experimental conditions as the bacterial pigment. It was employed

Downloaded from pubs.acs.org/acsodf/article-pdf/doi/10.1021/acsomega.6c03470/6922768l/acsomega.6c03470.pdf by ANADOLU UNIV. Pervin Soyer on 18 November 2026

https://doi.org/10.1021/acsomega.6c03470
ACS Omega XXXX, XXX, XXX−XXX

as a standardized comparative reference rather than as a structurally identical model of the microbial pigment, because chemically synthesized melanin may differ from biologically produced melanin in terms of polymer organization, degree of polymerization, and structural heterogeneity.

2.2. Instruments

pH measurements were performed using pH meters (OHAUS ST10 and Hanna PH211). Sterilization and incubation were carried out using an autoclave (Hirayama HVN-50), shaking incubator (Edmund Bühler TH 15), and drying oven (Binder FD53). A laminar flow cabinet (Heraeus HeraSafe) was used for aseptic procedures. Centrifugation and sonication were performed using an Eppendorf 5804R centrifuge and a Bandelin Sonorex ultrasonic bath, respectively. Spectrophotometric analyses were conducted using a NanoDrop spectrophotometer and a Cytation 3 multimode reader (BioTek). Molecular analyses were performed using PCR and sequencing systems (Applied Biosystems). Structural characterization of melanin was carried out using FT-IR spectroscopy (PerkinElmer Spectrum Two, ATR) and field emission scanning electron microscopy coupled with energy-dispersive X-ray spectroscopy (FE-SEM/EDS; Hitachi Regulus 8230, Japan). Cell culture studies were conducted in a CO_2 incubator (Thermo Scientific), and cell counting was performed using a Cedex XS analyzer.

2.3. Sampling Site and Sample Collection

Tuz Lake, located in a tectonic depression basin at the intersection of Ankara, Konya, and Aksaray provinces (Türkiye), is the second largest and one of the shallowest lakes in the country. During periods of intense evaporation, the salinity reaches up to 32%, classifying it among the hypersaline lakes worldwide. The lake water exhibits an alkaline character, with pH values typically ranging between 7.5 and 9.0.[11] Water samples were collected from Tuz Lake at coordinates 39°04′28.2″ N and 33°24′33.5″ E using sterile glass containers. Prior to sampling, the containers were rinsed thoroughly with lake water and then submerged and filled completely. The samples were transported to the laboratory under cold conditions and stored at 4 °C until further processing.

2.4. Isolation and Purification of Bacteria

Bacterial isolation from water sample was performed using the membrane filtration method. Briefly, 30 mL of each water sample was filtered through sterile cellulose nitrate membrane filters (pore size 0.45 μm), and the procedure was carried out in five replicates. After filtration, the membranes were placed onto isolation medium selective for melanin-producing bacteria, consisting of beef extract (3.0 g/L), peptone (5.0 g/L), yeast extract (10.0 g/L), NaCl (10.0 g/L), L-tyrosine (0.04 g/L), and agar (20.0 g/L) in distilled water (1 L). All cultures were incubated at 28 °C for 7 days. Following incubation, colonies exhibiting typical dark or black pigmentation were selected and purified by the streak plate method on freshly prepared isolation medium. The purified cultures were subsequently transferred into 20% (v/v) glycerol solution and stored at −20 °C for further use.[12,13]

2.5. Screening of Melanin-Producing Bacteria

Bacterial isolates obtained from Tuz Lake were screened for melanin production. For this purpose, cultures were inoculated into 100 mL of liquid melanin production medium consisted of beef extract (3.0 g/L), peptone (5.0 g/L), yeast extract (3.0 g/L), NaCl (5.0 g/L), L-tyrosine (0.12 g/L), and $CuSO_4$ (0.008 g/L) in distilled water (1 L) prepared in 250 mL Erlenmeyer flasks. Briefly, standardized bacterial suspension adjusted to approximately 1.5×10^8 CFU/mL (0.5 McFarland standard) was transferred into the medium and incubated in a shaking, illuminated incubator at 28 °C and 120 rpm for 7−10 days.[12,14] At the end of the incubation period, cultures exhibiting complete black pigmentation were considered as melanin-producing bacteria and selected for further studies.

2.6. Identification of Bacterial Isolate

Bacterial isolate was identified using both morphological and molecular approaches.

2.6.1. Morphological Identification. Gram staining was performed according to standard microbiological procedures to evaluate the Gram reaction and cellular morphology of the purified bacterial isolate. Stained cells were examined under a light microscope using oil immersion magnification (100× objective) and Gram reaction and cellular morphology were recorded.

2.6.2. Molecular Identification. The bacterial isolate was identified by 16S rRNA gene sequencing. Genomic DNA was extracted using a commercial bacterial DNA purification kit, and the 16S rRNA gene was amplified using universal primers 27F (5′-AGAGTTTGATCMTGGCTCAG-3′) and 1492R (5′-TACGGYTACCTTGTTACGACTT-3′) under standard PCR conditions. PCR products were purified and sequenced using an ABI 3730XL DNA analyzer (Applied Biosystems, USA). The obtained sequences were assembled into consensus sequences and compared with sequences available in the NCBI GenBank database using the BLAST algorithm for taxonomic identification.

2.7. Melanin Production and Extraction

Melanin production was carried out in liquid medium (Medium 3) consisting of beef extract (3.0 g/L), peptone (5.0 g/L), yeast extract (3.0 g/L), NaCl (5.0 g/L), L-tyrosine (0.12 g/L), and $CuSO_4$ (0.008 g/L) prepared in distilled water (1 L). Briefly, 100 mL of the medium was dispensed into 250 mL Erlenmeyer flasks and inoculated with a standardized bacterial suspension adjusted to approximately 1.5×10^8 CFU/mL (0.5 McFarland standard). The cultures were incubated in a shaking, illuminated incubator at 28 °C and 120 rpm for 7−10 days.[12,14] The cultures were incubated until dark pigmentation was observed. Uninoculated medium controls were incubated under the same conditions to exclude pigment formation originating from medium components or abiotic oxidation. Following incubation, bacterial cells were removed by centrifugation at 4000 rpm for 15 min, and the supernatant containing extracellular melanin was collected. Since the isolates produced melanin extracellularly, only the supernatant was used for further extraction. To precipitate melanin, the pH of the supernatant was adjusted to 1.8−2.0 using 6 M HCl and kept overnight to allow complete precipitation. Acid precipitation at pH 1.8−2.0 using HCl was performed according to commonly used microbial melanin extraction protocols reported in the literature. Melanin is known to possess considerable chemical stability under acidic conditions due to its highly cross-linked and heterogeneous polymeric structure. Similar acidic precipitation procedures have been widely used for microbial melanin recovery without causing significant structural degradation.[5,8] The precipitated melanin was recovered by centrifugation at 4000 rpm for 15 min and washed 3 to 4× with distilled water to remove impurities. The final precipitate was centrifuged again under the same conditions to obtain a black melanin pellet, which was subsequently dried at 60 °C for 24 h. The dried melanin extract was stored at 4 °C for further characterization and biological activity assays.[12]

2.8. Structural and Physicochemical Characterization of Melanin

2.8.1. Solubility Test. The solubility of the extracted melanin was evaluated in water, organic solvents, acidic, and alkaline solutions, including ethanol, methanol, acetone, chloroform, ethyl acetate, dimethyl sulfoxide (DMSO), 0.1 M NaOH, phosphate-buffered saline (PBS, pH 8), acetic acid, and 1 M HCl. Melanin dispersibility was assessed visually after mixing at room temperature.[15]

2.8.2. Spectrophotometric Analysis. The presence of melanin was confirmed by its characteristic absorption profile, showing maximum absorbance in the UV region. Melanin samples (1 mg) were dissolved in 1 mL of 0.1 M NaOH, and 10 μL of each solution was transferred into 96-well plates containing 190 μL of 0.1 M NaOH. Absorbance spectra were recorded in the range of 200−400 nm using a UV−vis multimode microplate reader (BioTek Synergy HTX, USA).[16] 0.1 M NaOH was used as a blank, and synthetic melanin was included as a reference standard. The obtained absorbance data were processed using OriginPro 2024b software, and spectral plots were generated for each melanin sample.

Downloaded from pubs.acs.org/acsodf/article-pdf/doi/10.1021/acsomega.6c03470/6922768l/acsomega.6c03470.pdf by ANADOLU UNIV. Pervin Soyer on 18 November 2026

https://doi.org/10.1021/acsomega.6c03470
ACS Omega XXXX, XXX, XXX−XXX

2.8.3. Functional Group Analysis (FT-IR). Fourier-transform infrared (FT-IR) spectroscopy was employed to identify functional groups present in the melanin structure. Melanin extract and synthetic melanin (4 mg) were analyzed using an FT-IR spectrometer (PerkinElmer Spectrum Two, USA) equipped with an attenuated total reflectance (ATR) unit over the wavenumber range of 500−4000 cm^{-1}. The obtained spectra were processed and visualized using SpectraGryph software (v1.2.16.1).

2.8.4. Differential Scanning Calorimetry Analysis. The thermal properties of synthetic and microbial melanin samples were evaluated using differential scanning calorimetry (DSC) (DSC-60, Shimadzu Scientific Instruments, Columbia, MI, USA). Approximately 5 mg of each sample was accurately weighed into aluminum pans and analyzed under a constant air flow of 50 mL min^{-1} at a heating rate of 10 °C min^{-1} over a temperature range of 30−300 °C. In addition to synthetic melanin used as a reference material, a microbial melanin sample obtained from a different *Bacillus atrophaeus* isolate was comparatively analyzed to evaluate the thermal behavior and stability characteristics of the melanin samples.[17−19]

2.8.5. Surface Morphology and Elemental Analysis. The surface morphology of melanin sample was examined using field emission scanning electron microscopy (FE-SEM), while elemental composition was determined by energy-dispersive X-ray spectroscopy (EDS). Analyses were performed using a Hitachi Regulus 8230 FE-SEM system equipped with an EDS detector. The sample was mounted on aluminum stubs and coated with a thin layer of gold/palladium (Au/Pd) for 120 s using a sputter coater (Leica EM ACE600, Germany). Morphological imaging and elemental mapping were subsequently performed under appropriate operating conditions.

2.8.6. ^{1}H NMR Analysis. ^{1}H NMR spectroscopy was performed to obtain additional structural information on the extracted melanin. Since the melanin sample was insoluble in common organic solvents but soluble under alkaline conditions, the melanin extract and synthetic melanin were dissolved in 0.1 M NaOD prepared in D_2O.[20] The 10 mg of melanin extract and synthetic melanin were dissolved in 600 μL of 0.1 M NaOD/D_2O by vortexing and transferred into a 5 mm NMR tube. The ^{1}H NMR spectrum was recorded at room temperature using a 400 MHz Bruker AVANCE III NMR spectrometer (Bruker Bioscience, Billerica, MA, USA) at 298 K (25 °C). Chemical shifts (δ) were referenced in parts per million (ppm) relative to the residual solvent signal. Owing to the heterogeneous, highly cross-linked, and amorphous nature of melanin, broad resonance signals were expected and interpreted according to previously reported microbial and synthetic melanin spectra.

2.9. Biological Activities of Melanin

2.9.1. Antimicrobial Activity. The antimicrobial activity of melanin extract was determined using the broth microdilution method, and minimum inhibitory concentration (MIC) values were calculated.[21−24] For this purpose, two Gram-positive bacteria (*Staphylococcus aureus* ATCC 29213 and *Bacillus subtilis* NRRL B478), two Gram-negative bacteria (*Escherichia coli* ATCC 25922 and *Pseudomonas aeruginosa* ATCC 27853), and two yeast species (*Candida albicans* ATCC 90028 and *Candida krusei* ATCC 6258) were used as test microorganisms. The selected bacterial and fungal strains represent clinically relevant Gram-positive, Gram-negative, and yeast microorganisms commonly used in antimicrobial susceptibility studies. Fresh cultures incubated at 37 °C for 24 h were adjusted to a turbidity equivalent to 0.5 McFarland standard (approximately 1.5 × 10^8 CFU/mL) using sterile physiological saline. Subsequently, bacterial suspensions were diluted to obtain final inoculum concentrations of 2.5−5 × 10^5 CFU/mL in Mueller−Hinton broth (MHB), while yeast suspensions were adjusted to 0.5−2.5 × 10^3 CFU/mL in Sabouraud dextrose broth (SDB), in accordance with CLSI guidelines. Melanin extract was prepared as stock solutions at a concentration of 5000 μg/mL in 0.1 M NaOH. In 96-well microplates, 100 μL of sterile distilled water was initially added to each well. Then, 100 μL of melanin extract was added to the first row and 2-fold serial dilutions were performed to obtain concentrations ranging from 1250 to 0.152 μg/mL. Afterward, 100 μL of the prepared microbial suspension was added to each well, and the plates were incubated at 37 °C for 24 h. Following incubation, 20 μL of 0.01% resazurin solution was added to each well, and the plates were further incubated for 2−4 h. A color change from blue to pink indicated microbial growth, whereas the retention of blue/purple color indicated inhibition of growth. The MIC value was defined as the lowest concentration at which no color change was observed. Standard antibiotics, including erythromycin (for Gram-positive bacteria), ciprofloxacin (for Gram-negative bacteria), and amphotericin B (for yeasts), were used as positive controls, while 0.1 M NaOH served as a negative control. All experiments were performed in triplicate.

2.9.2. Antioxidant Activity. The antioxidant activity of melanin extract was evaluated using the DPPH (2,2-diphenyl-1-picrylhydrazyl) radical scavenging assay.[25] For the antioxidant activity assay, 200 μL of each melanin extract was transferred into the first well of a 96-well microplate. Subsequently, 2-fold serial dilutions were performed by transferring 100 μL from each well into adjacent wells containing 100 μL of methanol. As a result, melanin extract, synthetic melanin, and ascorbic acid were tested at concentrations ranging from 625 to 39.0635 μg/mL. Then, 100 μL of DPPH solution (0.08 mg/mL) was added to each well, and the reaction mixtures were incubated in the dark at room temperature for 30 min. After incubation, absorbance values were measured at 517 nm using a microplate reader[21,26,27] The free radical scavenging activity of the sample was expressed as percentage inhibition using the following eq (eq 1)

$$\text{Inhibition } \% = [(A_{\text{control}} - A_{\text{sample}})/A_{\text{control}}] \times 100 \quad (1)$$

where A_{control} represents the absorbance of the control (without sample), and A_{sample} represents the absorbance of the test sample. IC_{50} values were determined from dose−response curves. Ascorbic acid and synthetic melanin were used as reference standards.

2.9.3. Cytotoxic Activity. The cytotoxic potential of melanin extract was assessed using the MTT assay.[28−32] HaCaT (Human adult, low Calcium, High Temperature keratinocyte) cell line (CLS, Germany, No: 300,493) was used as the model cell line. Cells were cultured in Dulbecco's Modified Eagle Medium (DMEM) supplemented with fetal bovine serum and penicillin/streptomycin under standard conditions (37 °C, 5% CO_2, and 95% relative humidity) until approximately 80% confluence was reached. Cells were detached using trypsin−EDTA, resuspended in fresh medium, and counted using a cell counter. Subsequently, cells were seeded into 96-well plates at a density of 5 × 10^3 cells per well in 100 μL of medium and incubated for 24 h to allow cell attachment. Melanin extract and synthetic melanin were prepared at concentrations of 62.5, 125, 250, 500, and 1000 μg/mL in 0.1 M NaOH and applied to the cells. After 24 h of incubation, 10 μL of MTT solution (5 mg/mL) was added to each well, and the plates were incubated for an additional 3 h. The medium was then carefully removed, and 100 μL of DMSO was added to dissolve the formazan crystals formed by metabolically active cells. Absorbance was measured at 540 nm using a microplate reader. Cell viability (%) was calculated using the following eq (eq 2)

$$\text{Inhibition } \% = [(A_{\text{control}} - A_{\text{sample}})/A_{\text{control}}] \times 100 \quad (2)$$

where A_{sample} represents the absorbance of melanin-treated cells and A_{control} represents untreated control cells. In addition, IC_{50} values were calculated from dose−response curves.

2.9.4. UV-Protective Activity. The UV-protective effect of melanin was evaluated to determine its ability to protect microorganisms against UV-induced damage. *Bacillus subtilis* and *Saccharomyces cerevisiae* were used as model organisms. *Bacillus subtilis* and *S. cerevisiae* were selected as representative prokaryotic and eukaryotic model microorganisms, respectively, to evaluate the UV-protective potential of melanin under different cellular systems. Microbial cultures were grown on appropriate media (MHA for bacteria and SDA for yeast) at 37 °C for 48 h. The cultures were diluted (10^{-4}) in sterile physiological saline, and 1 mL of each suspension was transferred into 24-well plates. Subsequently, 1 mL of melanin extract (1 mg/mL) was added to each well. The plates were

Downloaded from pubs.acs.org/acsodf/article-pdf/doi/10.1021/acsomega.6c03470/6922768l/acsomega.6c03470.pdf by ANADOLU UNIV. Pervin Soyer on 18 November 2026

https://doi.org/10.1021/acsomega.6c03470
ACS Omega XXXX, XXX, XXX−XXX

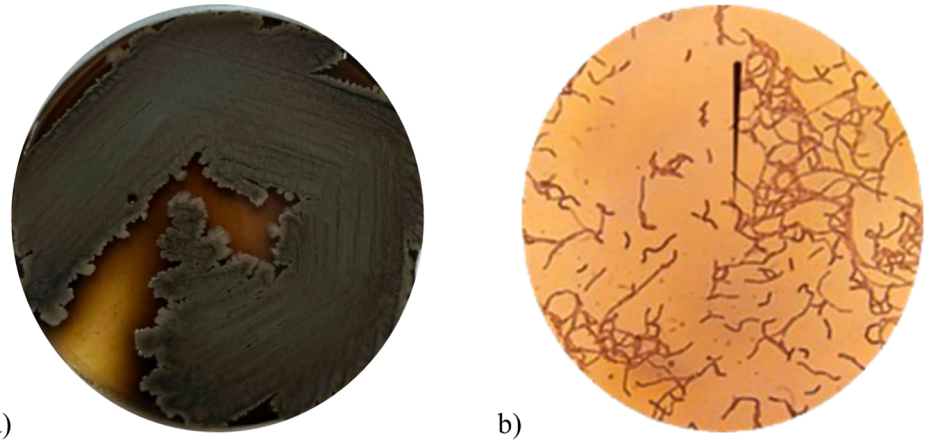


Figure 1. Morphological characteristics of the melanin-producing *Bacillus atrophaeus* strain 41 isolated from Tuz Lake. (a) Colony morphology showing intense black pigmentation on agar medium, indicative of melanin production. (b) Gram-stained microscopic image revealing Gram-positive, rod-shaped (bacillus) cells.

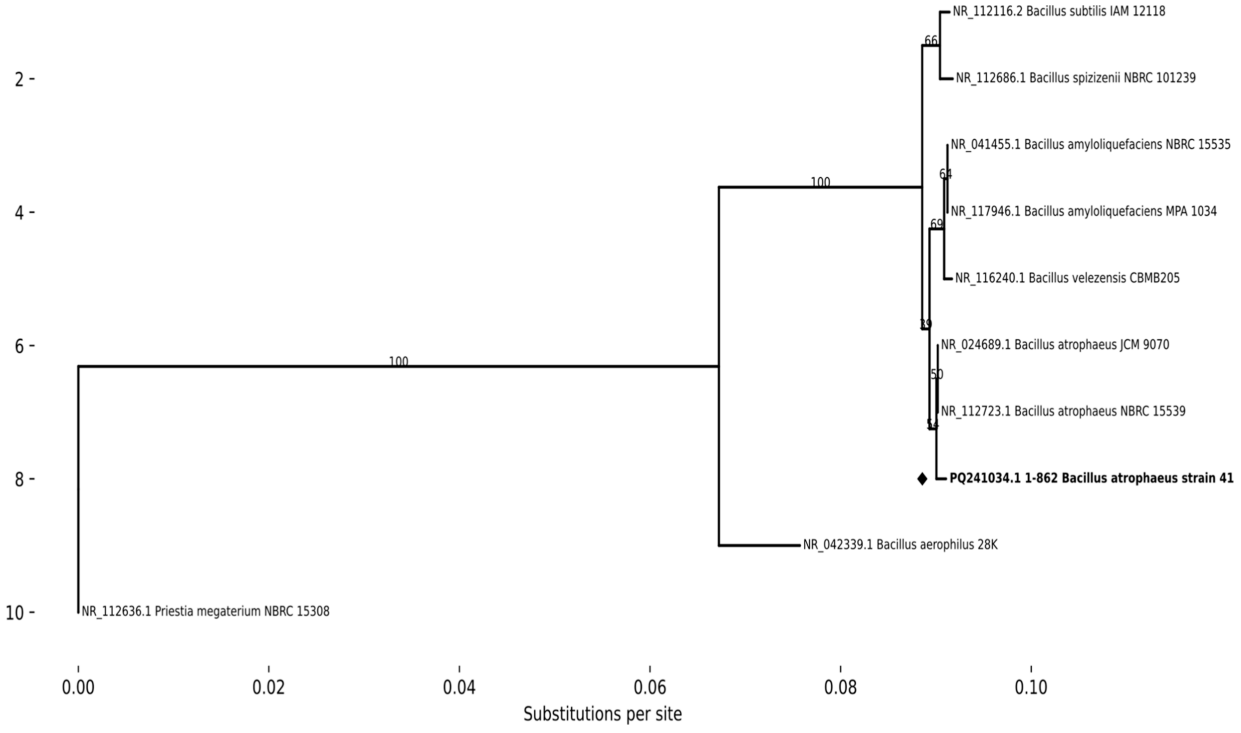


Figure 2. Phylogenetic tree based on 16S rRNA gene sequences showing the position of *Bacillus atrophaeus* strain (PQ241034.1) among closely related *Bacillus* species.

exposed to UV radiation (360 nm) from a distance of 33 cm for different time intervals (1, 3, 5, 10, and 20 min). Following UV exposure, 100 μL of each sample was spread onto agar plates and incubated at 37 °C for 48 h. The protective effect of melanin was evaluated based on microbial growth compared to control groups exposed and unexposed to UV radiation.[33,34]

2.10. Determination of Melanin Biosynthetic Pathway

The melanin biosynthetic pathway was investigated using specific pathway inhibitors. Kojic acid (10, 50, and 100 μg/mL) was used as an inhibitor of the DOPA pathway, while phthalide (10, 50, and 100 μg/mL) and tricyclazole (0.5, 1, and 2 μg/mL) were used to inhibit the DHN pathway.[35] These inhibitors were added to 100 mL of melanin production medium prior to inoculation. The cultures were incubated at 30 °C for 7 days, and pigment formation was monitored visually. The absence of black pigmentation indicated inhibition of melanin synthesis, whereas unchanged pigmentation suggested that the inhibitor had no effect on the biosynthetic pathway. To ensure that the inhibitors did not affect cell viability, cultures were subcultured onto nutrient broth (NB), and growth was monitored.

2.11. Optimization of Melanin Production

To enhance melanin production yield, culture medium components were optimized using a statistical experimental design approach. A Box−Behnken design (BBD), one of the most widely used response surface methodology (RSM) techniques, was employed to evaluate the effects of selected variables on melanin production. Carbon source, nitrogen source, L-tyrosine concentration, and metal salt concentration were selected as independent variables, while the extracted melanin yield was defined as the response variable. The experimental design consisted of four factors at three levels (−1, 0, +1), resulting in a total of 27 experimental runs. The design matrix and statistical analyses were generated and evaluated using Minitab software (Minitab Inc., USA). Nutrient broth (NB) was used as the

https://doi.org/10.1021/acsomega.6c03470
ACS Omega XXXX, XXX, XXX−XXX

Downloaded from pubs.acs.org/acsodf/article-pdf/doi/10.1021/acsomega.6c03470/6922768l/acsomega.6c03470.pdf by ANADOLU UNIV. Pervin Soyer on 18 November 2026

basal medium for all experiments, supplemented with NaCl, and the pH was adjusted to 8.0 prior to sterilization. Each experimental condition was prepared in 100 mL volumes and inoculated with a standardized bacterial suspension (1.2×10^9 CFU/mL). Cultures were incubated in a shaking, illuminated incubator at 30 °C and 120 rpm for 7 days. Following incubation, melanin extraction was performed using the previously described method, and the yield was determined gravimetrically by weighing the dried melanin extract. The obtained data were subjected to statistical analysis to determine the optimal conditions for maximum melanin production.

2.12. Statistical Analysis

Data obtained from antioxidant activity, UV-protective activity, and cytotoxicity assays were analyzed using GraphPad Prism software (version 8.0, GraphPad Software Inc., USA). Statistical comparisons were performed using one-way analysis of variance (ANOVA) followed by Tukey's post hoc test. All results are expressed as mean ± standard deviation (SD) of three independent experiments. Statistical significance was interpreted as follows: $p > 0.05$, not significant; $p < 0.05$ (*), significant; $p < 0.01$ (**), highly significant; $p < 0.001$ (***), very highly significant; and $p < 0.0001$ (****), extremely significant.

3. RESULTS AND DISCUSSION

3.1. Isolation, Screening, and Identification of Melanin-Producing Bacteria

Within the scope of this study, Tuz Lake, a hypersaline and polyextreme environment, was selected as the sampling site for the isolation of melanin-producing bacteria. Such environments are known to harbor extremophilic and stress-resistant microorganisms, which are more likely to produce protective pigments such as melanin, making hypersaline ecosystems promising niches for the discovery of novel pigment-producing strains. Following the isolation procedures, a bacterial isolate exhibiting intense black pigmentation was obtained from culture plates, suggesting potential melanin production. Since dark pigmentation is commonly associated with melanin synthesis in microorganisms, it was used as a primary screening criterion. Preliminary characterization of the isolate by Gram staining revealed a Gram-positive, rod-shaped (bacillus) morphology, consistent with members of the genus *Bacillus* (Figure 1). For precise taxonomic identification, molecular analysis based on 16S rRNA gene sequencing was performed. The obtained sequence (GenBank accession No. PQ241034.1) was compared with reference sequences in the NCBI GenBank database using the BLAST algorithm, revealing 100% sequence similarity with *Bacillus atrophaeus*. Phylogenetic analysis further supported this identification, showing that the isolate clustered within the *Bacillus subtilis* species complex and formed a well-supported clade with *Bacillus atrophaeus* reference strains. Closely related taxa included *Bacillus subtilis*, *Bacillus spizizenii*, and *Bacillus amyloliquefaciens*, reflecting the known genetic proximity within this group. Bootstrap values indicated the stability of the major nodes. However, due to the limited discriminatory power of the 16S rRNA gene within this complex, taxonomic assignment was interpreted in conjunction with sequence similarity data (Figure 2). *Bacillus atrophaeus*, previously reported under several synonyms such as *B. subtilis* var. *niger* and *Bacillus globigii*, is a Gram-positive, aerobic, spore-forming bacterium phenotypically similar to *B. subtilis*, but capable of pigment production under specific growth conditions.[10] The species is widely used as a biological indicator in sterilization processes and has applications in decontamination, agriculture, and biomolecule production.[36] In addition, it is known to produce antimicrobial compounds such as subtilosin A and has been investigated for its immunostimulatory potential.[37,38] Overall, these findings confirm that the melanin-producing isolate obtained from Tuz Lake belongs to *Bacillus atrophaeus*, highlighting this species as a promising source of microbial melanin. Moreover, its occurrence in a hypersaline environment suggests a potential adaptive role of melanin in protecting cells against environmental stress factors such as high salinity and radiation.

3.2. Melanin Production and Extraction

Melanin production was visually confirmed by the complete black pigmentation of the culture medium, indicating active melanogenesis by the bacterial isolate. Upon reaching maximum pigmentation, the production process was terminated, and melanin was extracted. The extraction of microbial melanin is primarily based on acid precipitation under strongly acidic conditions. Prior to precipitation, microbial cells were removed from the culture medium to obtain extracellular melanin present in the supernatant. Subsequently, melanin was precipitated by acidification, enabling its separation from soluble impurities.[39−41] The yield of the extracted microbial melanin was determined to be 158.0 mg/L. This relatively high production level indicates that the isolated *Bacillus atrophaeus* strain is an efficient melanin producer under the applied culture conditions. The ability of the isolate to produce extracellular melanin simplifies downstream processing and enhances its potential for large-scale production. The observed production efficiency highlights the suitability of this strain as a promising candidate for biotechnological applications requiring microbial melanin.

3.3. Structural and Physicochemical Characterization of Melanin

3.3.1. Solubility Test. The solubility analysis revealed that the produced melanin extract was soluble in 0.1 M sodium hydroxide (NaOH) and phosphate-buffered saline (PBS, pH 8), while remaining insoluble in water and organic solvents such as ethanol, methanol, acetone, chloroform, ethyl acetate, acetic acid, HCl, and DMSO. This behavior is consistent with the characteristic solubility profile of natural melanins. The solubility of melanin is strongly associated with the ionization state of its functional groups, particularly carboxyl groups.[42,43] Under alkaline conditions, deprotonation of these groups enhances the solubility of melanin by increasing its interaction with the solvent. In contrast, under neutral or acidic conditions, melanin remains largely insoluble due to its complex, heterogeneous, and highly cross-linked polymeric structure.[8] The observed insolubility of melanin in both aqueous and organic solvents is a well-documented feature of microbial and natural melanins, reflecting their predominantly hydrophobic and amorphous nature. Despite its apparent hydrophobicity, melanin contains various functional groups that contribute to its amphiphilic behavior under specific conditions. Upon dissolution in alkaline media, the melanin extract exhibited a characteristic dark black color and a viscous appearance, consistent with previous reports. This behavior can be attributed to the partial depolymerization of melanin aggregates into smaller oligomeric units at higher pH values. Such structural changes are likely driven by ionizable functional groups and intermolecular interactions within the polymer matrix.[44] The solubility profile of the obtained melanin is in good agreement with previously reported microbial melanins, further supporting its classification as a typical eumelanin-like biopolymer.

Downloaded from pubs.acs.org/acsodf/article-pdf/doi/10.1021/acsomega.6c03470/6922768l/acsomega.6c03470.pdf by ANADOLU UNIV. Pervin Soyer on 18 November 2026

https://doi.org/10.1021/acsomega.6c03470
ACS Omega XXXX, XXX, XXX−XXX

3.3.2. UV−Vis Spectrophotometric Analysis. Melanin is an amorphous pigment that exhibits a characteristic broad-band absorption in the UV−vis spectrum, often described as a "scattering phenomenon", arising from the superposition of multiple overlapping absorption peaks, known as the chemical disorder model.[45] This unique optical behavior is attributed to the heterogeneous and highly conjugated structure of melanin. The extracted melanin sample showed maximum absorbance at approximately 280 nm (Figure 3), which is consistent with the

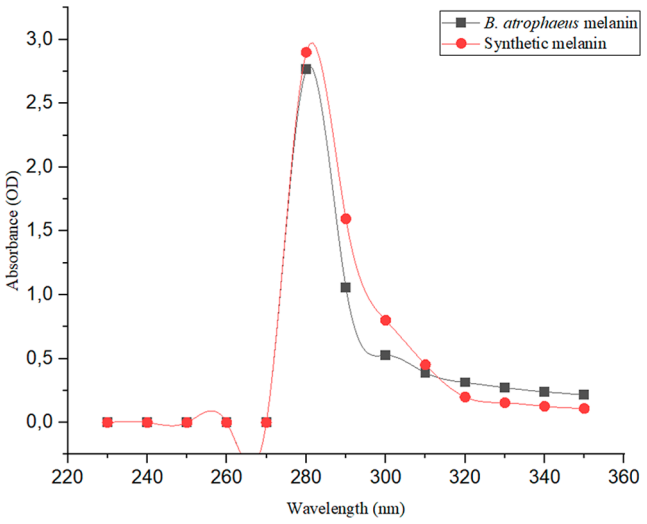


Figure 3. UV−vis absorption spectra of melanin extract obtained from *Bacillus atrophaeus* and synthetic melanin.

presence of aromatic, amino, and carboxylic functional groups.[46] Strong absorption in the UV region (200−300 nm) is a well-known characteristic of melanin and is directly related to its protective role against harmful radiation. In all analyzed samples, absorbance was highest in the UV region and gradually decreased toward the visible region as the wavelength increased. This monotonic decrease is a typical feature of melanin and reflects its complex conjugated polymeric structure. The progressive decline in absorbance with increasing wavelength is commonly linear when plotted on a logarithmic scale against wavelength, and the slope of this linear relationship has been widely used as a criterion for melanin characterization. Moreover, the absence of additional distinct absorption maxima above 280 nm suggests that no major UV-absorbing chromophores were evident under the applied analytical conditions; however, this observation alone does not establish chemical purity.[5,8] According to the literature, the absorption maxima of melanin typically fall within the range of 200−300 nm, depending on the biological source and solvent conditions.[47] Alkaline melanin solutions generally exhibit a continuous decrease in optical absorbance across the UV−vis spectrum (200−900 nm), further supporting the presence of a highly conjugated aromatic system. This absorption behavior is consistent with that of aromatic compounds and confirms the polymeric and heterogeneous nature of melanin.[48,49]

3.3.3. FT-IR Analysis of Functional Groups. FT-IR spectroscopy was employed to analyze the structural features of microbial melanin in comparison with synthetic melanin by identifying vibrational modes of functional groups and polar bonds within the molecule. Although slight variations in IR spectra may occur depending on the microbial source and extraction conditions, melanin exhibits characteristic absorption bands that allow identification of its main functional groups. The FT-IR spectra of both synthetic and extracted melanin sample revealed broad and intense absorption bands, reflecting the complex and heterogeneous nature of the melanin polymer. Such broad peaks arise from overlapping signals of multiple functional groups within the structure.[50] Detailed assignments of the observed wavenumbers and corresponding functional groups are presented in Tables 1

Table 1. FT-IR Peak Analysis of Synthetic Melanin

Wavenumber (cm^{-1})	Functional Group Assignment
3277	O−H stretching
2928	aliphatic C−H stretching
1616	C═O, C═C, C═N aromatic ring stretching or secondary N−H stretching
1553	N−H stretching
1488	N═O stretching or C−H stretching
1370	C−H and O−H stretching
1269	phenolic O−H stretching
1211	phenolic O−H stretching
1041	C−H stretching
796	aromatic C−H bending and C═C deformation

Table 2. FT-IR Peak Analysis of Melanin Obtained from *Bacillus atrophaeus*

Wavenumber (cm^{-1})	Functional Group Assignment
3149	O−H stretching
2989	aliphatic C−H stretching
2902	C−H stretching
1635	C═O, C═C, C═N aromatic ring stretching or secondary N−H stretching
1517	N−H stretching
1406	N═O stretching or C−H stretching
1230	phenolic O−H stretching
1066	aliphatic amine N═O stretching or phenolic −COOH
892	aromatic C−H bending and C═C deformation

and 2, while the FT-IR spectra are shown in Figure 4. Overall, the spectral profile of the extracted pigment was consistent with that of commercial synthetic melanin and supported the presence of functional groups commonly associated with melanin-like polymers. These bands are consistent with hydroxyl-, phenolic-, aromatic-, carbonyl-, and amine-associated functional groups reported for microbial melanin-like materials, although FT-IR alone cannot provide definitive subtype identification.

The FT-IR spectra of melanin obtained from *Bacillus atrophaeus* isolates exhibited characteristic absorption bands consistent with those of standard melanin. The observed peaks correspond to O−H stretching, aliphatic C−H stretching, aromatic ring vibrations (C═C, C═N) or secondary N−H stretching, N−H stretching, N═O or C−H stretching, phenolic O−H stretching, aliphatic amine or phenolic −COOH groups, and aromatic C−H bending and C═C deformation. These functional groups are typical of melanin and confirm its complex, heterogeneous polymeric structure. Comparative analysis with literature further supports these

Downloaded from pubs.acs.org/acsodf/article-pdf/doi/10.1021/acsomega.6c03470/6922768l/acsomega.6c03470.pdf by ANADOLU UNIV. Pervin Soyer on 18 November 2026

https://doi.org/10.1021/acsomega.6c03470
ACS Omega XXXX, XXX, XXX−XXX

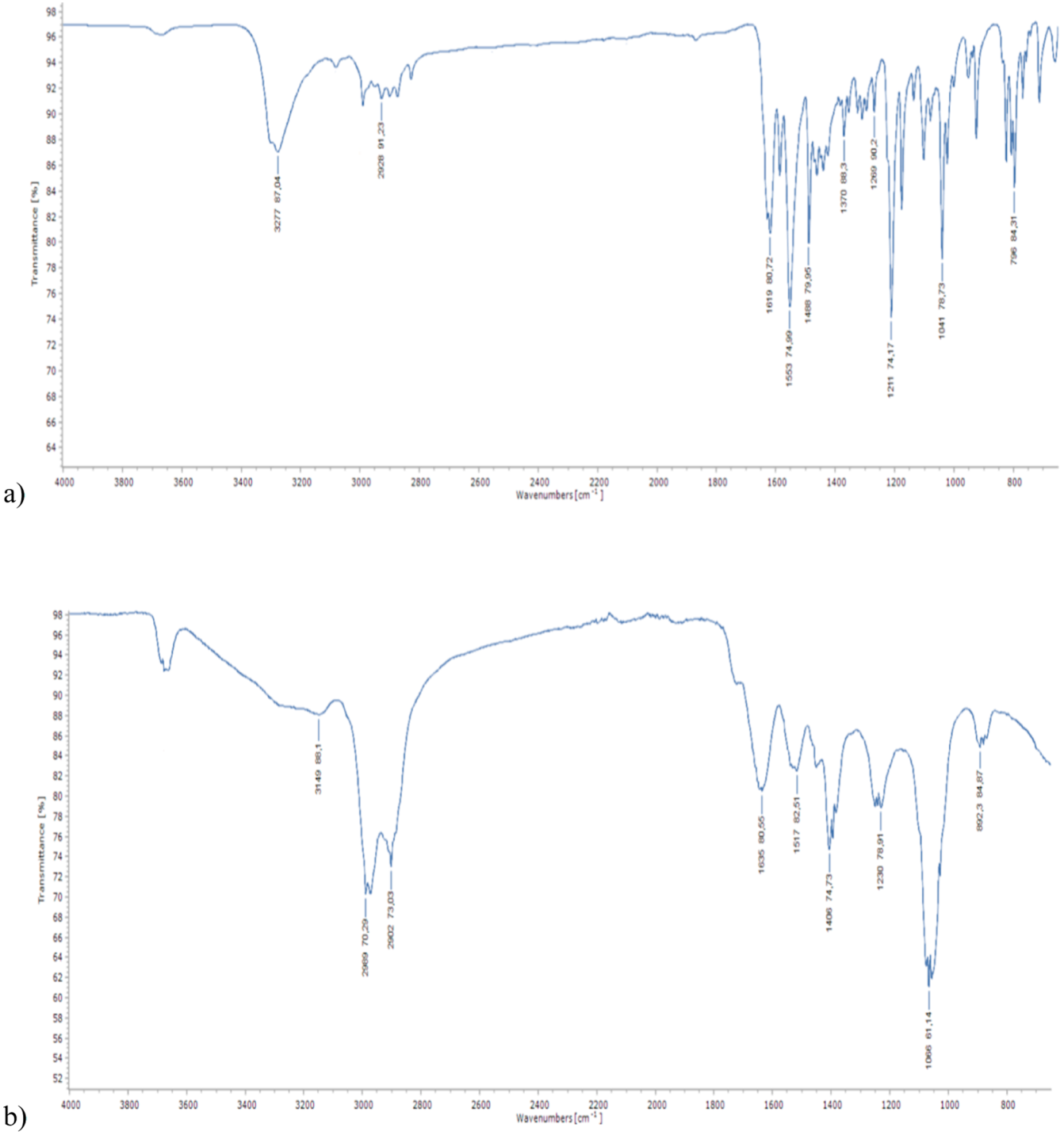


Figure 4. FT-IR spectra of (a) synthetic melanin and (b) melanin extracted from *Bacillus atrophaeus*.

findings. Melanin obtained from *Bacillus weihenstephanensis* showed similar FT-IR peaks at 3268, 2970, 1622, 1517, 1438, 1220, 1045, and 874 cm^{-1},[51] while melanin derived from *Streptomyces glaucescens* exhibited characteristic peaks at 3421, 2947, 1647, 1539, 1423, 1240, 1058, and 864 cm^{-1}.[5] These wavenumbers correspond to similar functional groups, including hydroxyl, aliphatic, aromatic, and amine-related vibrations, indicating a conserved structural pattern among microbial melanins. Notably, the absorption band observed at approximately 2902 cm^{-1}, attributed to C−H stretching, was present in the melanin extracted from *B. atrophaeus* but absent in the synthetic melanin spectrum. This difference may indicate structural variations between natural and synthetic melanin, possibly related to the presence of additional aliphatic or protein-associated components in microbial melanin. Additionally, in some microbial melanin sample, this band has been associated with both C−H and N−H stretching vibrations, suggesting a more complex chemical environment within the polymer matrix. These findings highlight subtle structural differences while overall confirming that the obtained melanin exhibits typical eumelanin-like characteristics.

Downloaded from pubs.acs.org/acsodf/article-pdf/doi/10.1021/acsomega.6c03470/6922768l/acsomega.6c03470.pdf by ANADOLU UNIV. Pervin Soyer on 18 November 2026

https://doi.org/10.1021/acsomega.6c03470
ACS Omega XXXX, XXX, XXX−XXX

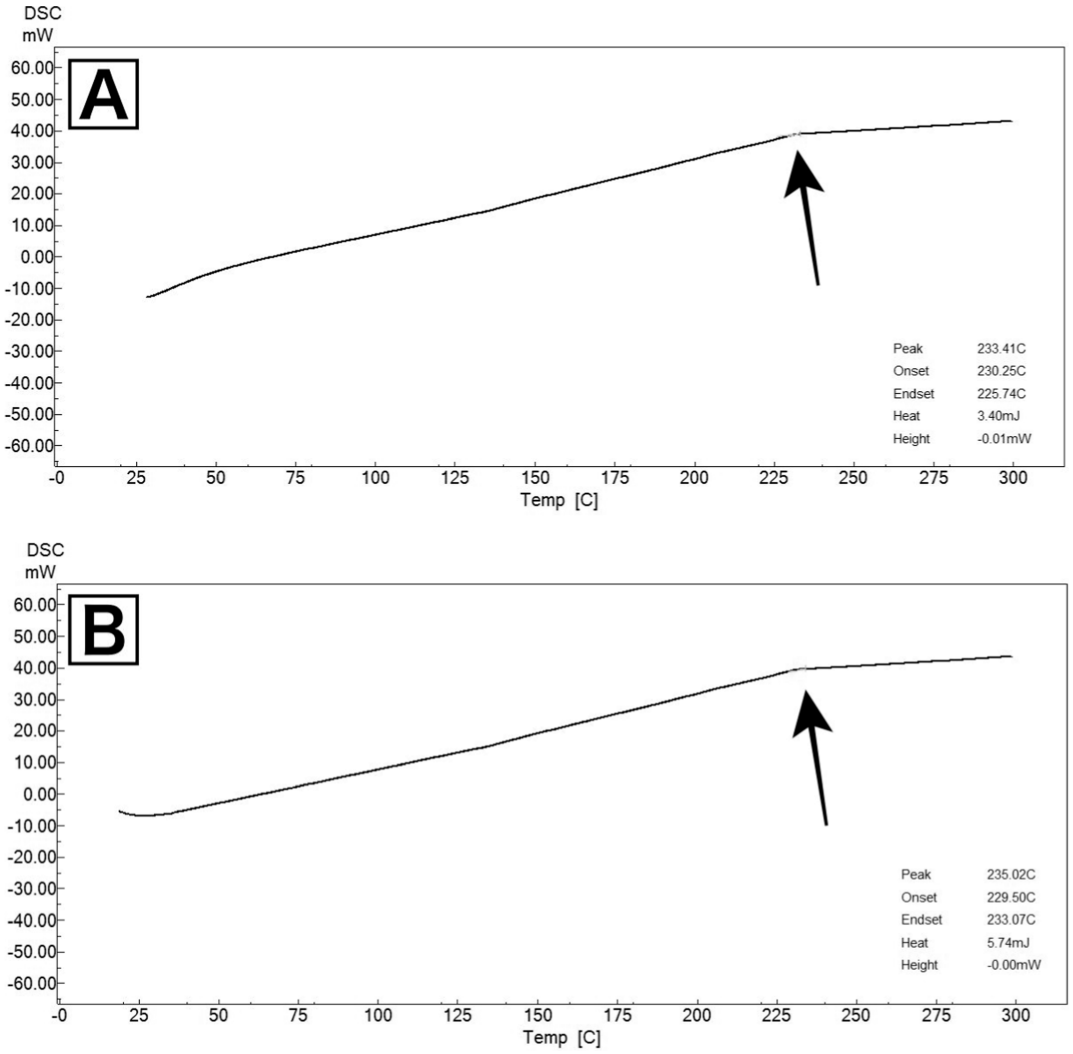


Figure 5. Differential scanning calorimetry (DSC) thermograms of (A) synthetic melanin and (B) bacterial melanin extracted from *Bacillus atrophaeus*.

3.3.4. Differential Scanning Calorimetry Analysis. The obtained DSC results and thermal transition temperatures of synthetic and microbial melanin samples are presented in Figure 5. The DSC thermograms of synthetic and microbial melanin did not exhibit a sharp and distinct endothermic melting peak, indicating the predominantly amorphous, heterogeneous, and highly cross-linked polymeric nature of melanin.[52,53] This behavior is consistent with the characteristic thermal properties of eumelanin-like biopolymers reported in the literature. Instead of classical crystalline melting, broad low-enthalpy thermal transitions associated with structural relaxation and thermal decomposition were observed.[21] Synthetic melanin exhibited a thermal transition at approximately 233.41 °C, whereas microbial melanin sample showed transition at 235.02 °C. The microbial sample demonstrated high thermal stability, with a transition temperature slightly higher than that of synthetic melanin. This finding suggests the presence of a more condensed and structurally organized melanin network with stronger intermolecular interactions, improved aromatic conjugation, and enhanced polymeric stability. The superior thermal stability of microbial sample is particularly important for potential pharmaceutical, cosmetic, and biotechnological applications, as higher thermal resistance may contribute to improved stability during formulation, processing, sterilization, and storage. Therefore, the DSC findings further support that the melanin produced by *Bacillus atrophaeus* strain possesses a highly stable eumelanin-like structure with favorable physicochemical characteristics.[54,55]

3.3.5. Elemental Composition of Melanin (EDS Analysis). The surface morphology of synthetic and bacterial melanin was examined by scanning electron microscopy (SEM), while the elemental composition was determined by energy-dispersive X-ray spectroscopy (EDS). SEM observations revealed that both synthetic melanin and melanin extracted from *Bacillus atrophaeus* exhibited irregular, amorphous aggregates, which is a characteristic feature of melanin structures reported in the literature. The micrographs demonstrated the presence of small, rough, and spherical-like particles forming aggregated structures (Figure 6), consistent with previously reported microbial melanins.[56,57] This morphology reflects the heterogeneous, noncrystalline, and highly polymerized nature of melanin.

The elemental composition of melanin extracted from *B. atrophaeus* and synthetic melanin is presented in Table 3. The microbial melanin was primarily composed of carbon (62.33%) and oxygen (12.29%), confirming its organic and polymeric

Downloaded from pubs.acs.org/acsodf/article-pdf/doi/10.1021/acsomega.6c03470/6922768l/acsomega.6c03470.pdf by ANADOLU UNIV. Pervin Soyer on 18 November 2026

https://doi.org/10.1021/acsomega.6c03470
ACS Omega XXXX, XXX, XXX−XXX

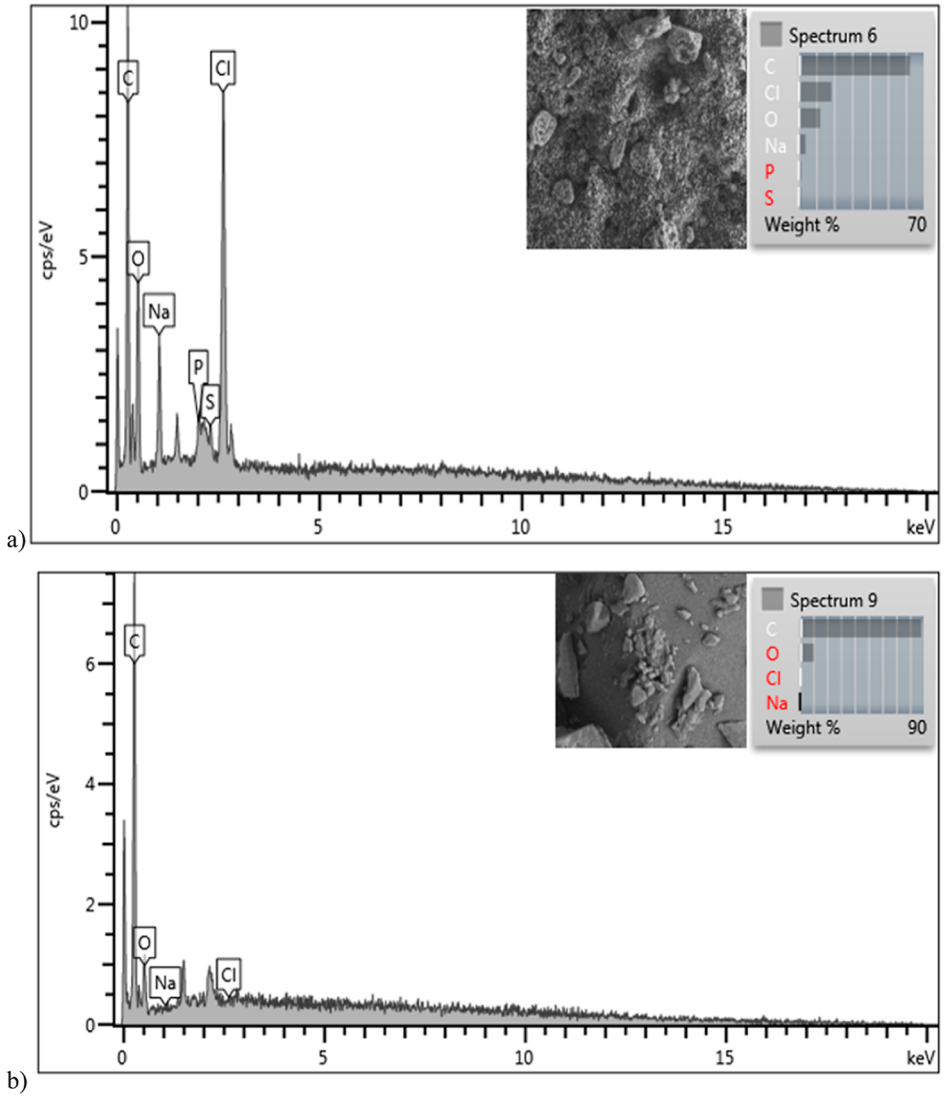


Figure 6. SEM images and EDS spectra of melanin samples: (a) *Bacillus atrophaeus*-derived melanin and (b) synthetic melanin.

Table 3. Elemental Composition (%) of Melanin Extract

Samples	C	O	Na	Cl	Al	P	S	K	N	Si	Ca
B. atrophaeus **extract**	62.33	12.29	4.01	18.58	-	1.52	1.37	-	-	-	
synthetic melanin	88.28	10.34	0.26	1.12	-	-	-	-	-	-	

structure. These results are consistent with the known structure of melanin, which consists of highly conjugated aromatic carbon frameworks containing oxygen-bearing functional groups such as hydroxyl and carboxyl groups. Compared to microbial melanin, synthetic melanin exhibited a significantly higher carbon content (88.28%) and lower proportions of other elements, indicating a more homogeneous and purified composition. The relatively lower carbon content observed in microbial melanin suggests the presence of additional inorganic ions or residual biomolecules associated with its biological origin and extraction process. A notable finding was the relatively high chlorine content (18.58%) together with sodium (4.01%) in *B. atrophaeus*-derived melanin. These elements are most likely linked to the hypersaline origin of the isolate (Tuz Lake) and the salt-rich culture conditions. Such ionic residues are commonly reported in melanins produced by halotolerant microorganisms and may influence their physicochemical properties. The relatively high chlorine signal observed in the EDS spectrum is most likely associated with residual salt ions originating from the hypersaline environment and saline culture conditions rather than being structurally integrated into the melanin backbone. Since the producing strain was isolated from Tuz Lake, an extreme hypersaline ecosystem, the adsorption or retention of sodium and chloride ions within the heterogeneous melanin matrix is plausible. Previous studies have similarly reported the presence of inorganic ions in melanins produced by halotolerant microorganisms, particularly when extracted under high-salinity conditions.[58,59] The polyanionic and amorphous nature of melanin enables ionic interactions and binding with environmental cations and anions, which may contribute to the detected elemental composition.[2,8] Additionally, trace amounts of phosphorus (1.52%) and sulfur (1.37%) were detected, suggesting the possible presence of

Downloaded from pubs.acs.org/acsodf/article-pdf/doi/10.1021/acsomega.6c03470/6922768l/acsomega.6c03470.pdf by ANADOLU UNIV. Pervin Soyer on 18 November 2026

https://doi.org/10.1021/acsomega.6c03470
ACS Omega XXXX, XXX, XXX−XXX

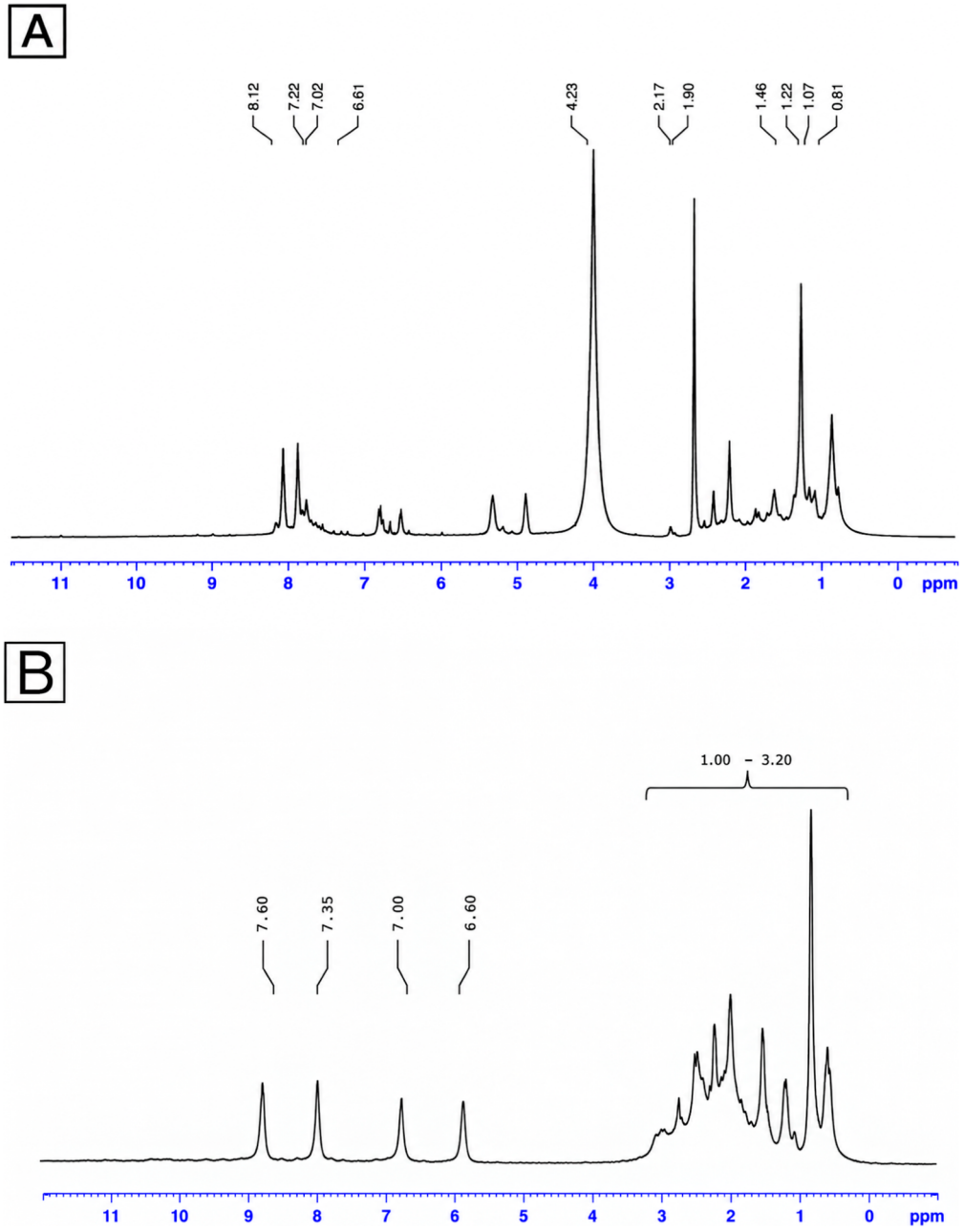


Figure 7. ^{1}H NMR spectra of melanin samples. (A) Synthetic melanin used as the reference standard and (B) melanin extracted from the halotolerant *Bacillus atrophaeus* isolate.

protein-associated residues or sulfur-containing functional groups within the melanin structure. Potassium, nitrogen, silicon, and calcium were not detected under the applied EDS conditions. However, nondetection should not be interpreted as definitive absence, particularly for light elements such as nitrogen, for which conventional SEM−EDS has limited sensitivity. Nitrogen emits a relatively low-energy characteristic X-ray signal, and its detection may be affected by detector sensitivity, accelerating voltage, sample geometry, matrix effects, signal-to-noise ratio, and elemental concentration. Consequently, low levels of nitrogen present within heterogeneous organic polymers may remain below the practical detection limit of EDS. Therefore, the absence of a detectable nitrogen signal is not sufficient to exclude the presence of nitrogen-containing indolic structures within the pigment. Confirmation of nitrogen content would require complementary techniques such as CHNS elemental analysis or X-ray photoelectron spectroscopy (XPS). Although sulfur was detected at a relatively low level (1.37 wt %) in the EDS analysis, its origin cannot be determined from elemental analysis alone. The detected sulfur may originate from residual sulfur-containing proteins or peptides, cysteine- or methionine-containing cellular components, culture medium constituents, inorganic sulfur-containing residues retained during purification, environmental contaminants, purification-related artifacts, or minor sulfur-containing structures associated with the pigment itself. Because EDS provides only semiquantitative elemental composition and does not provide information on chemical bonding, oxidation state, or molecular structure, it cannot determine whether the detected sulfur is structurally

Downloaded from pubs.acs.org/acsodf/article-pdf/doi/10.1021/acsomega.6c03470/6922768l/acsomega.6c03470.pdf by ANADOLU UNIV. Pervin Soyer on 18 November 2026

https://doi.org/10.1021/acsomega.6c03470
ACS Omega XXXX, XXX, XXX−XXX

incorporated into the melanin polymer or originates from external sources. Therefore, the sulfur signal alone cannot be used either to confirm or to exclude sulfur-containing melanin structures. Consequently, while the combined inhibitor profile, UV−vis, FT-IR, and ^{1}H NMR findings are most consistent with a predominantly DOPA-dependent eumelanin-like pigment, the presence of a minor sulfur-containing melanin component or a heterogeneous eumelanin−pheomelanin-like composition cannot be conclusively excluded. Definitive discrimination would require complementary techniques such as melanin-specific chemical degradation, CHNS elemental analysis, X-ray photoelectron spectroscopy (XPS), electron paramagnetic resonance (EPR), or solid-state NMR. When compared with literature data, the elemental composition of the obtained melanin shows similarity to sepia melanin derived from *Sepia officinalis*, reported to contain 55.49% carbon, 7.14% nitrogen, 6.19% sodium, 4.02% chlorine, 1.67% magnesium, 1.01% calcium, and 0.14% potassium.[60] Although variations are expected depending on the biological source and environmental conditions, this similarity supports the classification of the obtained pigment as a typical microbial melanin. Overall, SEM revealed an amorphous and aggregated morphology comparable to that commonly reported for natural melanin-like materials, while EDS demonstrated a carbon- and oxygen-rich elemental profile with additional minor elements. These findings are compatible with a heterogeneous microbial melanin-like pigment but are not sufficient on their own to establish a specific melanin subtype.

3.3.6. ^{1}H NMR Spectroscopy Analysis. To provide additional structural evidence supporting the proposed biosynthetic pathway, the extracted pigment was further characterized by ^{1}H NMR spectroscopy and compared with commercially available synthetic melanin (Figure 7). Although melanin is an inherently heterogeneous, highly cross-linked, and amorphous biopolymer, its proton NMR spectrum provides valuable information regarding the presence of aromatic, phenolic, and aliphatic structural motifs associated with different melanin types. Because eumelanin possesses a highly polymerized indole-based backbone, its spectra are generally characterized by broad and overlapping resonances rather than sharp, well-resolved signals, reflecting structural disorder and extensive π-electron delocalization. This behavior has been widely reported for both synthetic and microbial melanins.[2,8]

The synthetic melanin spectrum (Figure 7A) exhibited characteristic resonances within the aromatic region (δ 6.61−8.12 ppm), corresponding to indolic and aromatic protons that constitute eumelanin. Similar aromatic resonances have been consistently reported for synthetic eumelanin and Sepia melanin and are considered characteristic signatures of DOPA-derived melanin polymers.[2,43] In addition, several resonances between δ 0.8 and 2.2 ppm were observed, which are generally attributed to residual aliphatic side chains or minor nonaromatic components associated with the heterogeneous polymer network. The intense resonance around δ 4.23 ppm mainly corresponds to residual solvent (HDO) arising from the D_2O/NaOD system and therefore was not considered structurally significant. The *Bacillus atrophaeus*-derived melanin (Figure 7B) exhibited a spectral profile closely resembling that of the synthetic standard. Distinct aromatic resonances were observed at δ 6.60, 7.00, 7.35, and 7.60 ppm. These signals are consistent with conjugated aromatic environments and may include indole-related structural motifs commonly reported in DOPA-dependent eumelanin-like materials. However, owing to the heterogeneous and highly polymerized nature of melanin, the broad and overlapping resonances do not permit definitive assignment of individual monomeric units or unequivocal subtype identification. These signals are consistent with previously reported microbial melanins produced by *Streptomyces*, *Bacillus*, and *Pseudomonas* species, in which proton resonances between approximately δ 6.5 and 8.0 ppm have been attributed to polymerized indole and pyrrolic structures formed during DOPA oxidation.[5,61] The preservation of this aromatic region strongly supports the formation of an indole-based polymeric backbone. Compared with the synthetic melanin, the *Bacillus atrophaeus*-derived melanin exhibited a broader and more complex signal envelope within the δ 0.8−3.2 ppm region. Besides the intrinsic heterogeneity of naturally biosynthesized melanin, this increased spectral complexity may also be associated with the environmental origin of the producing strain. The isolate was recovered from the hypersaline ecosystem of Tuz Lake, where prolonged adaptation to high salinity, intense solar radiation, desiccation, and osmotic stress may promote the biosynthesis of structurally more heterogeneous melanin polymers. Such environmental adaptation has been suggested to influence melanin polymerization, molecular organization, and the incorporation of associated biomolecules, resulting in broader NMR resonances compared with synthetic melanin. The presence of sodium and chlorine detected by EDS analysis supports the interaction of the melanin matrix with ions characteristic of hypersaline environments, which may further contribute to its structural complexity. Nevertheless, additional high-resolution structural analyses, such as solid-state ^{13}C NMR and two-dimensional NMR spectroscopy, would be required to fully elucidate these structural variations. Importantly, no clearly resolved resonances that could be specifically assigned to sulfur-containing benzothiazine or benzothiazole structures, which are commonly associated with pheomelanin, were observed. However, the absence of such resolved signals in the ^{1}H NMR spectrum is not sufficient to exclude the presence of a minor sulfur-containing component, particularly because the pigment is heterogeneous and EDS detected sulfur (1.37 wt %). Likewise, no spectral features characteristic of DHN-derived naphthalene-type structures were observed. Therefore, the NMR findings are interpreted as being more consistent with a predominantly DOPA-dependent eumelanin-like aromatic structure, while the presence of a minor sulfur-containing fraction or heterogeneous eumelanin−pheomelanin-like composition cannot be conclusively excluded. These NMR findings are consistent with the biosynthetic inhibition experiments, in which pigment production was completely suppressed by kojic acid, a tyrosinase inhibitor, whereas tricyclazole and phthalide showed no inhibitory effect. When considered together, these complementary findings support the involvement of a DOPA-dependent biosynthetic pathway. However, they should be regarded as supportive rather than definitive evidence for classifying the pigment as a DOPA-dependent eumelanin-like material. The NMR findings were consistent with the complementary physicochemical analyses performed in this study. FT-IR confirmed the presence of hydroxyl, phenolic, aromatic C═C/C═N, and amine-related functional groups, while UV−vis exhibited the characteristic monotonic absorbance profile of highly conjugated melanin polymers. SEM revealed the typical amorphous aggregated morphology of

Downloaded from pubs.acs.org/acsodf/article-pdf/doi/10.1021/acsomega.6c03470/6922768l/acsomega.6c03470.pdf by ANADOLU UNIV. Pervin Soyer on 18 November 2026

https://doi.org/10.1021/acsomega.6c03470
ACS Omega XXXX, XXX, XXX−XXX

Table 4. Minimum Inhibitory Concentration (MIC, μg/mL) Values of *Bacillus atrophaeus*-Derived Melanin, Synthetic Melanin, and Reference Antimicrobial Agents against Selected Bacterial and Fungal Strains

Samples	*P. aeruginosa* ATCC 27853	*E. coli* ATCC 25922	*S. aureus* ATCC 29213	*B. subtilis* NRRL B478	*C. albicans* ATCC 90028	*C. krusei* ATCC 6258
***B. atrophaeus* extract**	312.50	312.50	312.50	312.50	625.00	625.00
synthetic melanin	625.00	625.00	625.00	625.00	625.00	625.00
erythromycin	-	-	1.25	1.25	-	-
ciprofloxacin	1	0.015	-	-	-	-
amphotericin B	-	-	-	-	0.5	1

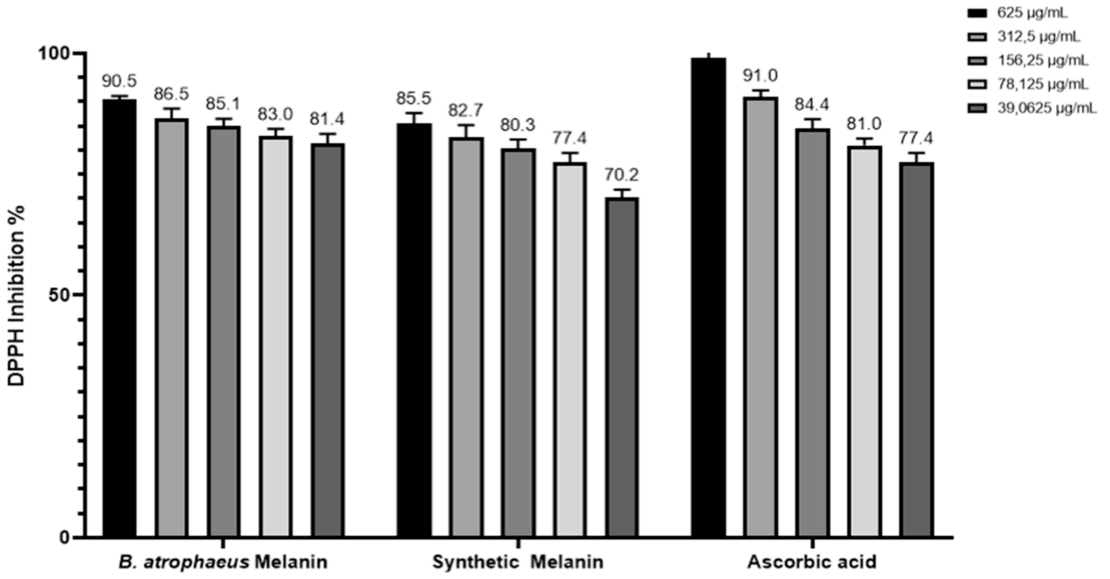


Figure 8. DPPH radical scavenging activity (%) of melanin extract and synthetic melanin at different concentrations. A significant increase in antioxidant activity was observed in a concentration-dependent manner (****$p < 0.0001$).

melanin, whereas EDS demonstrated a carbon- and oxygen-rich composition with minor amounts of sodium and chlorine, likely reflecting adaptation to the hypersaline environment. Furthermore, DSC indicated high thermal stability comparable to that of commercial synthetic melanin, supporting the presence of a highly cross-linked aromatic polymeric network. Collectively, the UV−vis, FT-IR, ^{1}H NMR, DSC, SEM, and EDS analyses indicate that the pigment produced by *Bacillus atrophaeus* shares physicochemical and structural characteristics with a DOPA-dependent eumelanin-like pigment. The similarities between the extracted pigment and commercial synthetic melanin, together with the kojic acid inhibition results, provide complementary evidence supporting the involvement of a tyrosinase-mediated DOPA biosynthetic pathway. Although the combined UV−vis, FT-IR, ^{1}H NMR, DSC, SEM, EDS, and biosynthetic inhibition analyses strongly support classification of the extracted pigment as a DOPA-dependent eumelanin-like pigment, they do not definitively establish its precise molecular composition or exclude the presence of minor sulfur-containing components. Future studies employing electron paramagnetic resonance (EPR), solid-state NMR, X-ray photoelectron spectroscopy (XPS), targeted chemical degradation, and other high-resolution structural techniques will be valuable for further elucidating the molecular architecture and confirming the precise melanin subtype.

3.4. Biological Activities of Melanin

3.4.1. Antimicrobial Activity. Natural products are widely recognized as important sources for the discovery of novel antimicrobial agents. In this study, the antimicrobial activity of melanin extract was evaluated using the broth microdilution method, and minimum inhibitory concentration (MIC) values were determined (Table 4).

The MIC values of both microbial melanin and synthetic melanin were found to be 625 and 312.5 μg/mL. Melanin extracted from *Bacillus atrophaeus* exhibited antimicrobial activity at lower concentrations (312.5 μg/mL) against bacterial test organisms, whereas all isolates showed similar activity against *Candida* species at 625 μg/mL. These findings indicate that the antibacterial activity of the microbial melanin is more pronounced than its antifungal activity. Comparative analysis with previous studies demonstrates that the melanin obtained in this study exhibits relatively strong antimicrobial activity. For instance, melanin produced by *Rhizobium radiobacter* has been reported to exhibit MIC values of 1500 μg/mL against *E. coli*, 2000 μg/mL against *S. aureus*, and 3500 μg/mL against *C. albicans*.[62] Similarly, melanin derived from *Pseudomonas mosselii* showed antimicrobial activity at considerably higher MIC values, including 3120 μg/mL for *E. coli*, 25,000 μg/mL for *Staphylococcus hemolyticus*, and 6250 μg/mL for *Listeria monocytogenes*. Compared to these reports, the lower MIC values observed in the present study suggest that *B. atrophaeus*-derived melanin possesses relatively higher antimicrobial potency. Synthetic melanin exhibited antimicrobial activity at 625 μg/mL against the tested microorganisms. Notably, microbial melanin extract demonstrated activity at lower concentrations than synthetic melanin, supporting the notion that naturally derived melanins may exhibit enhanced

Downloaded from pubs.acs.org/acsodf/article-pdf/doi/10.1021/acsomega.6c03470/6922768l/acsomega.6c03470.pdf by ANADOLU UNIV. Pervin Soyer on 18 November 2026

https://doi.org/10.1021/acsomega.6c03470
ACS Omega XXXX, XXX, XXX−XXX

bioactivity. The MIC values obtained in this study were lower than those reported for melanins produced by *R. radiobacter* and *P. mosselii*. Although the obtained MIC values are higher than those of conventional antibiotics, such concentrations are commonly reported for natural biopolymers and microbial melanins. Therefore, the observed activity levels remain biologically relevant and support the antimicrobial potential of the obtained melanin. The antimicrobial activity of melanin can be attributed to its chemical structure, particularly the presence of phenolic functional groups identified in FT-IR analysis. These groups are known to contribute to antimicrobial effects by denaturing microbial proteins. Additionally, the aromatic structure of melanin may disrupt microbial cell membranes or interact with intracellular targets such as proteins and DNA, leading to inhibitory effects.[63] It should be noted that antimicrobial activity may vary depending on the concentration of melanin, the type of test microorganisms, and the structural characteristics of the pigment. Variations in melanin structure, influenced by microbial origin and biosynthetic pathways, may lead to differences in biochemical mechanisms of action. Furthermore, the presence of residual impurities in the extracted melanin may also contribute to variations in MIC values. Overall, the relatively low MIC values obtained in this study indicate that *B. atrophaeus*-derived melanin exhibits promising antimicrobial activity and may serve as a potential candidate for future biotechnological and pharmaceutical applications. However, detailed mechanistic investigations such as ROS generation assays, membrane permeability studies, and ultrastructural analyses were beyond the scope of the present study and should be addressed in future research.

3.4.2. Antioxidant Activity. Melanin is a multifunctional pigment with physicochemical properties that make it highly suitable for biomedical applications. Due to the presence of unpaired electrons within its structure, melanin can act as both an electron donor and acceptor, enabling it to interact readily with free radicals and exhibit antioxidant activity.[5,63] The antioxidant activity of melanin extract was evaluated using the DPPH radical scavenging assay at concentrations ranging from 625 to 39.0625 μg/mL. The results were expressed as percentage inhibition of DPPH radicals and IC_{50} values (Figure 8 and Table 5). The *Bacillus atrophaeus*-derived melanin exhibited strong antioxidant activity, reaching 90.5% inhibition at the highest concentration (625 μg/mL). As the concentration decreased, the inhibition values gradually declined to 86.5%, 85.1%, and 83.0% at 312.5, 156.25, and 78.125 μg/mL, respectively. At the lowest concentration (39.0625 μg/mL), the melanin extract still maintained a relatively high scavenging activity of 81.4%. The IC_{50} value of *Bacillus atrophaeus*-derived melanin (82.26 μg/mL) was slightly higher than that of ascorbic acid (75.66 μg/mL) and synthetic melanin (74.86 μg/mL), indicating comparable antioxidant activity. Despite this slight difference, the microbial melanin demonstrated strong radical scavenging capacity, supporting its potential as an effective natural antioxidant. Although ascorbic acid showed slightly higher activity at equivalent concentrations (100−78% inhibition across the tested range), the results suggest that the bacterial melanin possesses a similarly strong radical scavenging capacity.

Table 5. IC_{50} Values (μg/mL) of Melanin Extract, Synthetic Melanin, and Ascorbic Acid Determined by the DPPH Radical Scavenging Assay

Samples	IC_{50} (μg/mL)
B. atrophaeus **extract**	82.26
Ascorbic acid	75.66
Synthetic melanin	74.86

Comparison with literature further supports these findings. For example, commercial melanin derived from *Sepia officinalis* exhibited 50% inhibition at 170.3 μg/mL,[64] which is significantly higher than the IC_{50} values obtained in this study. Similarly, melanin produced by *Streptomyces puniceus* demonstrated 89% inhibition at 100 μg/mL, compared to 96% for ascorbic acid at the same concentration. In another study, melanin from *Pseudomonas stutzeri* showed comparable antioxidant activity to synthetic melanin, with approximately 50−51% inhibition at 140 μg/mL.[65] Furthermore, melanin derived from *Bacillus subtilis* has been reported to exhibit strong antioxidant activity, with 94% inhibition at 100 μg/mL, surpassing ascorbic acid (86%) at the same concentration.[20] Similarly, melanin from *Bacillus safensis* showed higher inhibition than ascorbic acid within the 15−100 μg/mL range, with an IC_{50} value of 80.4 μg/mL.[66] These findings collectively support the strong antioxidant potential of Bacillus-derived melanins. Overall, the melanin extracted from *B. atrophaeus* demonstrated antioxidant activity comparable to or exceeding that of synthetic melanin and approaching that of ascorbic acid. This high antioxidant capacity is attributed to the presence of hydroxyl and aromatic functional groups within the melanin structure, which facilitate hydrogen donation and stabilization of DPPH radicals.[61]

3.4.3. Cytotoxic Activity. For the application of natural products in pharmaceutical and cosmetic fields, their safety profile and lack of cytotoxic effects are of critical importance.[67] Since melanin is primarily intended for skin-related applications, its cytotoxic effects on human keratinocytes are particularly relevant. In this study, the cytotoxicity of bacterial melanin extract was evaluated on HaCaT (immortalized human keratinocyte) cells, a widely used model in dermatological and toxicological research due to its ability to mimic human skin responses to environmental stressors such as UV radiation and chemical exposure.[68] The cytotoxic effects of melanin were assessed using the MTT assay over a concentration range of 1000 to 62.5 μg/mL. Cell viability (%) and IC_{50} values were determined (Figure 9 and Table 6). The results demonstrated that the *Bacillus atrophaeus*-derived melanin did not exhibit significant cytotoxic effects within the tested concentration range. The IC_{50} value of the bacterial melanin extract was calculated as 720.20 μg/mL, indicating low cytotoxicity and good biocompatibility. In comparison, synthetic melanin showed an even higher IC_{50} value (1022 μg/mL), suggesting slightly lower cytotoxic potential. However, the difference between microbial and synthetic melanin may be attributed to the presence of residual impurities in the extracted melanin, as no advanced purification techniques were applied. Such impurities may influence cytotoxic responses either positively or negatively. Notably, cell viability remained above 50% at concentrations of 250 μg/mL and below, indicating that the melanin extract is safe at lower concentrations relevant for potential applications.

These findings are consistent with previous studies reporting that melanin exhibits low cytotoxicity and may even provide protective effects against oxidative stress and UV-induced damage.[2] Similar observations have been reported in the

Downloaded from pubs.acs.org/acsodf/article-pdf/doi/10.1021/acsomega.6c03470/6922768l/acsomega.6c03470.pdf by ANADOLU UNIV. Pervin Soyer on 18 November 2026

https://doi.org/10.1021/acsomega.6c03470
ACS Omega XXXX, XXX, XXX−XXX

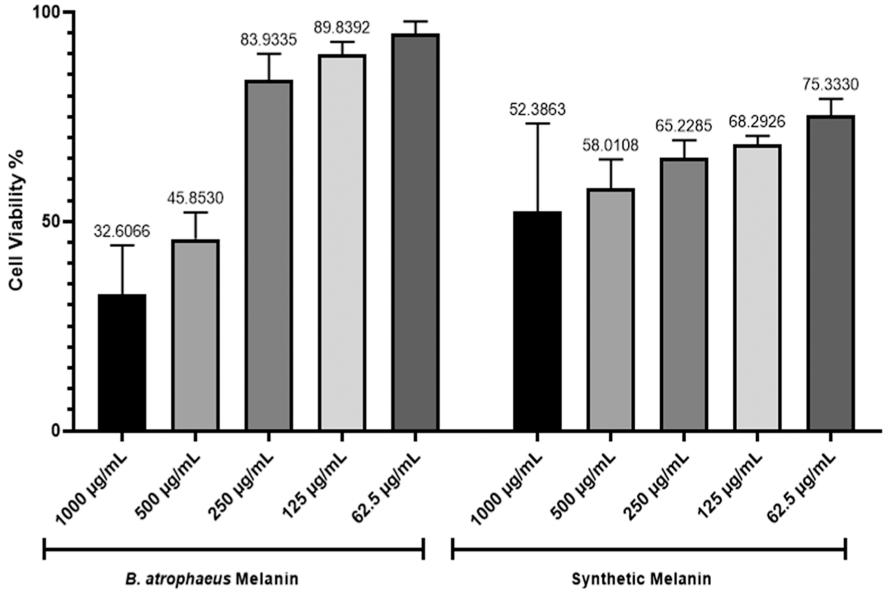


Figure 9. Cytotoxicity of melanin extract and synthetic melanin expressed as viability (%) (***$p < 0.001$).

Table 6. IC_{50} Values (μg/mL) of *Bacillus atrophaeus*-Derived Melanin and Synthetic Melanin against HaCaT Cells Determined by the MTT Assay

Samples	IC_{50} (μg/mL)
B. atrophaeus **extract**	720.20
Synthetic melanin	1022.20

literature. For instance, melanin produced by *Amorphotheca resinae* showed no cytotoxic effect on HaCaT cells up to 72 h of exposure, although cytotoxicity was observed at prolonged exposure (96 h) and higher concentrations (400 μg/mL).[69] The presence of functional groups such as phenolic −OH, aromatic structures, and C═O/C═N and N═O groups may contribute to dose-dependent biological effects, including potential cytotoxicity at higher concentrations. These groups

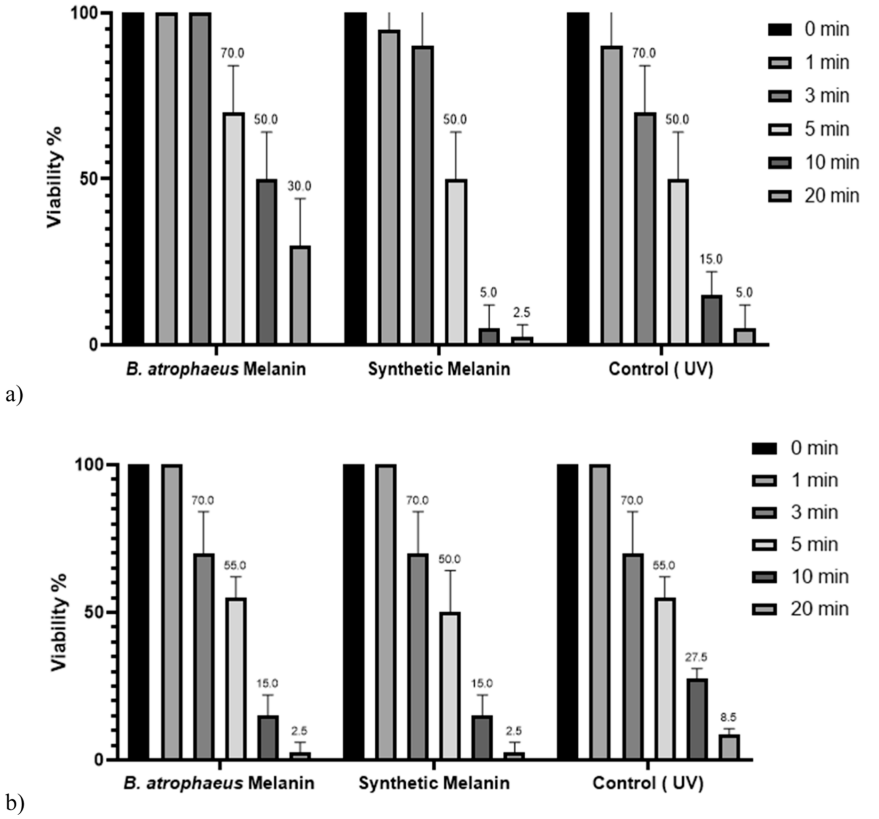


Figure 10. Percentage viability (%) demonstrating the UV-protective activity in (a) *Bacillus subtilis* NRRL B478 and (b) *Saccharomyces cerevisiae*. A highly significant difference was observed in both models (****$p < 0.0001$).

https://doi.org/10.1021/acsomega.6c03470
ACS Omega XXXX, XXX, XXX−XXX

Downloaded from pubs.acs.org/acsodf/article-pdf/doi/10.1021/acsomega.6c03470/6922768l/acsomega.6c03470.pdf by ANADOLU UNIV. Pervin Soyer on 18 November 2026

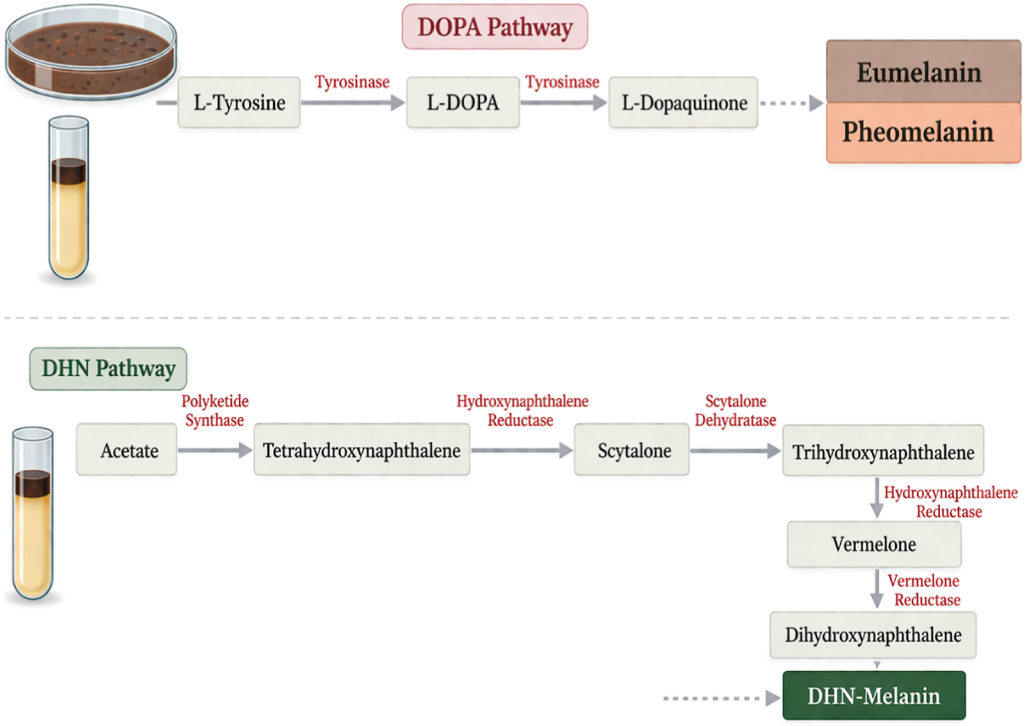


Figure 11. Schematic representation of microbial melanin biosynthesis pathways. The DOPA pathway involves the conversion of L-tyrosine to L-DOPA and subsequently to L-dopaquinone, leading to the formation of eumelanin and pheomelanin. The DHN pathway proceeds from acetate through polyketide intermediates to form DHN-melanin.

are known to influence cellular interactions by inducing oxidative stress or triggering controlled cell death mechanisms such as apoptosis. Therefore, the cytotoxic behavior of melanin is highly dependent on concentration, exposure time, and cell type.[3] These results indicate that *B. atrophaeus*-derived melanin exhibits low cytotoxicity and favorable biocompatibility, supporting its potential for safe use in biomedical, cosmetic, and pharmaceutical applications.

3.4.4. UV-Protective Activity. Microorganisms have evolved various adaptive mechanisms to survive under environmental stress conditions such as UV radiation. Pigment-producing microorganisms, in particular, exhibit significantly higher survival rates under UV exposure compared to nonpigmented counterparts, highlighting the evolutionary advantage conferred by pigments such as melanin. Microbially produced melanin functions as a protective barrier against oxidative stress and UV-induced cellular damage by absorbing UV radiation and scavenging reactive oxygen species (ROS). In this study, the UV-protective activity of melanin extract was evaluated by exposing model microorganisms to UV radiation (360 nm) for different time intervals (0, 1, 3, 5, 10, and 20 min). *Bacillus subtilis* and *S. cerevisiae* were selected as representative prokaryotic and eukaryotic models, respectively. Cell viability (%) was determined based on colony counts following UV exposure (Figure 10).

UV exposure led to a time-dependent decrease in microbial viability, primarily due to DNA damage such as thymine dimer formation, which interferes with DNA replication and cellular metabolism.[70] At early exposure times (1 min), DNA damage was limited, and repair mechanisms remained effective, resulting in relatively high survival rates (approximately 80−90%). However, prolonged exposure resulted in progressive accumulation of DNA damage, leading to a sharp decline in viability. After 3 min, survival decreased to around 50%, while at 5 and 10 min, viability dropped to 20−30% and 5−10%, respectively. At 20 min, survival rates were reduced to nearly 1%. Notably, melanin-treated cells exhibited enhanced resistance to UV radiation. The melanin extract derived from *B. atrophaeus* effectively protected *B. subtilis* cells up to 3 min of UV exposure without significant loss in viability, whereas in *S. cerevisiae*, protection was observed up to 1 min. Compared to untreated controls, melanin-treated cells maintained higher survival rates, demonstrating the protective capacity of the pigment. When compared with synthetic melanin, the microbial melanin extract showed superior UV-protective performance, suggesting that structural heterogeneity and functional group diversity in biologically produced melanin may enhance its photoprotective properties. Previous studies have similarly reported that melanin-containing microorganisms exhibit increased resistance to UV radiation. For instance, *B. atrophaeus* spores have been shown to possess intrinsic UV resistance due to their pigmentation.[71] Likewise, pigment-producing isolates such as *Flavobacterium* sp. and *Brevibacterium* sp. demonstrated significantly higher UV tolerance compared to nonpigmented *E. coli*, and extracted pigments were shown to confer UV protection when applied externally.[72] The observed UV-protective effect can be attributed to the chemical structure of melanin. Functional groups such as phenolic −OH, aromatic rings, conjugated systems, carbonyl (C═O), and imine (C═N) structures enable efficient absorption of UV radiation and dissipation of absorbed energy. Additionally, aliphatic groups contribute to the structural stability of the melanin matrix under irradiation.[3] The results demonstrate that *B. atrophaeus*-derived melanin possesses strong UV-protective properties, which are closely associated with its antioxidant capacity and structural features. These findings highlight its potential application as a natural

https://doi.org/10.1021/acsomega.6c03470
ACS Omega XXXX, XXX, XXX−XXX

Downloaded from pubs.acs.org/acsodf/article-pdf/doi/10.1021/acsomega.6c03470/6922768l/acsomega.6c03470.pdf by ANADOLU UNIV. Pervin Soyer on 18 November 2026

photoprotective agent in cosmetic and biomedical formulations.

3.5. Determination of Melanin Biosynthetic Pathway

Microbial melanins vary depending on the producing microorganism. Based on their biosynthetic pathways, microbial melanins are generally classified as DOPA-melanin and DHN-melanin. In the DOPA-melanin pathway, the key enzyme is tyrosinase. Tyrosinase oxidizes L-tyrosine to L-DOPA and then to L-dopaquinone, resulting in the formation of DOPA-type melanins such as eumelanin or pheomelanin. In the DHN-melanin pathway, the reaction begins with acetate as a precursor and proceeds through a series of reactions initiated by the polyketide synthase enzyme, ultimately forming DHN-melanin (Figure 11).

The type of melanin produced by microorganisms is generally determined using two approaches. The first involves the addition of melanin precursors to the culture medium, and the second involves the addition of inhibitors of melanin biosynthesis to the medium in order to predict the pathway. In this study, the second method, which provides more reliable results, was employed by using inhibitor agents to suppress melanin biosynthesis. Kojic acid, tricyclazole, and phthalide—specific inhibitors of DOPA and DHN melanin synthesis—were added to the production medium and tested on the producing microorganisms. It is important that the selected inhibitor does not inhibit the growth of the microorganism but only inhibits melanin production. Kojic acid inhibits the activity of tyrosinase, the enzyme responsible for DOPA-melanin synthesis.[35,73] Tricyclazole and phthalide inhibit the enzymatic reduction of DHN-melanin intermediates, specifically the conversion of scytalone and vermelone. Inhibition of melanin production in the presence of tricyclazole and phthalide indicates that the melanin may be produced via the DHN pathway. Conversely, the inhibition of melanin production by kojic acid supports the involvement of a predominantly DOPA-dependent biosynthetic pathway in pigment formation; however, this finding alone does not permit assignment of the pigment to a specific melanin subtype. The formation of black or dark coloration in inhibitor-containing media indicates melanin production, whereas the absence of dark coloration indicates inhibition of melanin synthesis due to the effect of the inhibitor. Considering that inhibitor agents may affect microbial growth, three different concentrations of each inhibitor were used (Table 7).

For the isolate belonging to *Bacillus atrophaeus*, it was observed that melanin production did not occur in the presence of kojic acid at all tested concentrations, whereas melanin production continued in the presence of tricyclazole and phthalide at different concentrations. Additionally, viability controls confirmed that all three inhibitors at all tested concentrations did not affect bacterial growth. Based on kojic acid inhibition together with UV−vis, FT-IR, DSC, SEM−EDS, and elemental composition analyses, the extracted pigment was considered to be a eumelanin-like melanin or pheomelanin-like melanin synthesized through the DOPA-melanin biosynthesis pathway. In a study conducted with *Klebsiella* sp., it was reported that melanin production was inhibited by kojic acid at a concentration of 30 μg/mL. This result was interpreted as evidence that the melanin pigment produced by *Klebsiella* sp. is synthesized via the DOPA-melanin pathway and resembles typical melanins with potential applications in cosmetics and pharmaceutical industries.[74] In another study, it was reported that sodium azide at 6.5 μg/mL, used as a DOPA pathway inhibitor, caused inhibition of melanin production in *Bacillus weihenstephanensis*. It was also observed that higher concentrations of sodium azide inhibited bacterial growth.[51] Pigment production by *B. atrophaeus* was completely inhibited by kojic acid at all tested concentrations, whereas tricyclazole and phthalide did not suppress pigmentation. Viability controls confirmed that the tested inhibitor concentrations did not prevent bacterial growth. This inhibition pattern supports the involvement of a tyrosinase-mediated DOPA pathway rather than a DHN-dependent pathway. However, pathway inhibition alone cannot distinguish eumelanin from pheomelanin because both pigment classes may arise from DOPA-related intermediates. Accordingly, pigment classification was based on the combined interpretation of the inhibitor profile, UV−vis, FT-IR, ^{1}H NMR, DSC, SEM−EDS, and comparison with commercial synthetic melanin. The predominance of broad aromatic resonances and the overall physicochemical similarity to the synthetic reference are more consistent with a predominantly eumelanin-like material. Nevertheless, because sulfur was detected by EDS and the available analyses cannot determine its chemical form or structural location, a minor sulfur-containing melanin component or heterogeneous pigment composition cannot be conclusively excluded. Therefore, the extracted material is described throughout this study as a DOPA-dependent eumelanin-like pigment rather than as definitively identified eumelanin.

Table 7. Qualitative Evaluation of Melanin Production by *Bacillus atrophaeus* in the Presence of Pathway-Specific Inhibitors (Tricyclazole, Phthalide, and Kojic Acid)

Inhibitors	Concentration (μg/mL)	*B. atrophaeus* melanin production
tricyclazole	**2**	+
	1	+
	0,5	+
phthalide	**100**	+
	50	+
	10	+
kojic acid	**100**	-
	50	-
	10	-
control (without inhibitor)	+	
inferred biosynthetic pathway	DOPA-dependent pathway	

3.6. Melanin Production Optimization

Melanin production was optimized using the Box−Behnken design, a response surface methodology (RSM) approach, to evaluate the effects of four independent variables: glucose (5−15 g/L), yeast extract (5−15 g/L), L-tyrosine (100−300 mg/L), and $CuSO_4$ (10−30 mg/L). The concentration ranges of glucose, yeast extract, L-tyrosine, and $CuSO_4$ used in the Box−Behnken design were determined based on previously reported melanin optimization studies involving bacterial and halotolerant microbial strains.[12,13,57,74] These factors were selected because they are known to directly influence melanin biosynthesis, microbial growth, and tyrosinase activity. The tested concentration ranges were chosen to ensure sufficient pigment production while avoiding possible substrate inhib-

Downloaded from pubs.acs.org/acsodf/article-pdf/doi/10.1021/acsomega.6c03470/6922768/acsomega.6c03470.pdf by ANADOLU UNIV. Pervin Soyer on 18 November 2026

Table 8. Experimental Design Matrix and Corresponding Melanin Production Yields (mg/L) Obtained Using Box−Behnken Design for *Bacillus atrophaeus*

Order no	Glucose g/L	Yeast extract g/L	Tyrosine mg/L	Copper sulfate mg/L	*B. atrophaeus* melanin mg/L	Predicted yield (mg/L)	Residual
1	10	15	100	20	1363	1348	15
2	10	10	200	20	1277	1261	16
3	15	10	200	10	1243	1258	−15
4	15	10	300	20	1276	1291	−15
5	15	10	100	20	1382	1367	15
6	5	10	100	20	927	944	−17
7	10	5	200	30	1110	1095	15
8	5	10	300	20	768	782	−14
9	10	15	200	10	1180	1166	14
10	5	10	200	30	888	903	−15
11	10	5	100	20	1224	1210	14
12	10	15	300	20	990	1005	−15
13	10	5	200	10	1116	1101	15
14	10	10	200	30	1728	1710	18
15	10	10	200	20	866	882	−16
16	10	10	300	30	1224	1209	15
17	15	10	200	30	1247	1230	17
18	10	10	100	10	1267	1250	17
19	5	10	200	20	907	922	−15
20	10	5	200	20	1159	1145	14
21	5	5	200	20	1068	1052	16
22	5	10	200	10	895	910	−15
23	10	5	300	20	948	963	−15
24	10	10	100	30	1773	1752	21
25	10	10	200	20	990	1002	−12
26	10	10	300	10	918	934	−16
27	15	15	200	20	1084	1068	16

Table 9. Analysis of Variance (ANOVA) Results for the Quadratic Regression Model of Melanin Production Optimization by Box−Behnken Design

Sources	Standard Deviation (SD)	Sum of Squares (SS)	Mean Square (MS)	*F*-value	*p*-value
model	14	1095272.000	78234.000	2.190	0.090
linear	4	771460.000	192865.000	5.400	0.025
glucose (G)	1	312987.000	312987.000	8.760	0.012
yeast extract	1	32761.000	32761.000	0.920	0.357
tyrosine (T)	1	273612.000	273612.000	7.660	0.017
$CuSO_4$	1	152100.000	152100.000	4.260	0.061
quadratic	4	232149.000	58037.000	1.630	0.231
glucose × glucose	1	26289.000	26289.000	0.740	0.408
yeast extract × yeast extract	1	18513.000	18513.000	0.520	0.485
tyrosine × tyrosine	1	35679.000	35679.000	1.000	0.337
$CuSO_4$ × $CuSO_4$	1	151668.000	151668.000	4.240	0.059
interaction	6	91663.000	15277.000	0.430	0.837
glucose × yeast extract	1	1849.000	1849.000	0.050	0.827
glucose × tyrosine	1	702.000	702.000	0.020	0.891
glucose × $CuSO_4$	1	30.000	30.000	0.001	0.977
yeast extract × tyrosine	1	2352.000	2352.000	0.070	0.802
yeast extract × $CuSO_4$	1	76729.000	76729.000	2.150	0.168
tyrosine × $CuSO_4$	1	10000.099	10000.099	0.280	0.606
error	12	428517.000	35710.000		
total	26	1523789.000			

ition effects at higher precursor concentrations. A total of 27 experimental runs were conducted under controlled conditions (30 °C, 120 rpm, 7 days), and melanin yields were determined following extraction. The experimental design matrix and corresponding melanin yields are presented in Table 8. The results demonstrated considerable variation in melanin production depending on medium composition. The highest melanin yield (1.773 g/L) was obtained at 10 g/L glucose, 10 g/L yeast extract, 100 mg/L L-tyrosine, and 30 mg/L $CuSO_4$, indicating the critical role of balanced nutrient composition in pigment biosynthesis.

Analysis of variance (ANOVA) results (Table 9) showed that the linear model was statistically significant ($p = 0.025 < 0.05$), confirming that the selected variables significantly

https://doi.org/10.1021/acsomega.6c03470
ACS Omega XXXX, XXX, XXX−XXX

Downloaded from pubs.acs.org/acsodf/article-pdf/doi/10.1021/acsomega.6c03470/6922768l/acsomega.6c03470.pdf by ANADOLU UNIV. Pervin Soyer on 18 November 2026

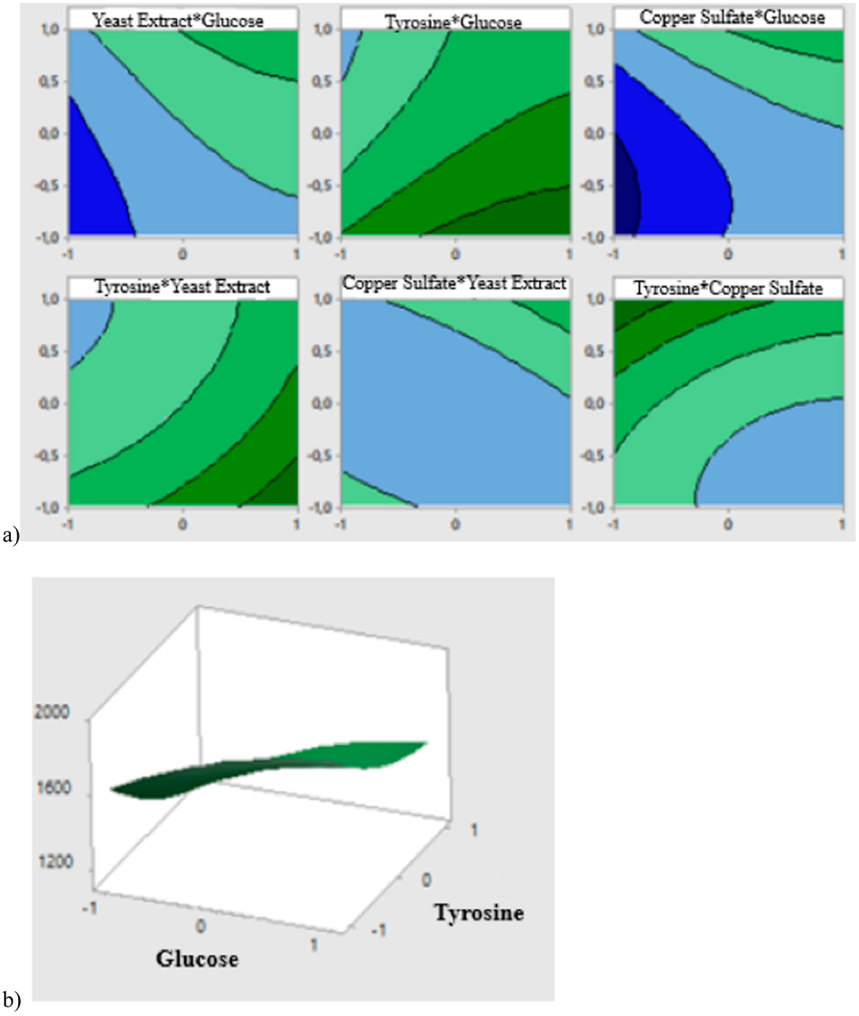


Figure 12. Response surface analysis of melanin production by *Bacillus atrophaeus*. (a) Contour plots showing the interactive effects of yeast extract, glucose, tyrosine, and copper sulfate on melanin yield. (b) Three-dimensional response surface plot illustrating the combined effect of glucose and tyrosine on melanin production.

influenced melanin production. Among the tested factors, glucose ($p = 0.012$) and L-tyrosine ($p = 0.017$) were identified as statistically significant contributors, whereas yeast extract and $CuSO_4$ showed no significant individual effects ($p > 0.05$). Quadratic and interaction terms were generally not significant, suggesting that melanin production is primarily influenced by linear effects of key variables rather than complex interactions.

The regression model demonstrated a coefficient of determination (R^2) of 71.88% and an adjusted R^2 of 70.17%, indicating a good agreement between predicted and experimental values. The regression model describing melanin production (Y, mg/L) as a function of the independent variables is given as follows (eq 3).

$$Y = 1044 + 161.5G + 52.3M - 151.0T + 112.6B - 70.2G^2 + 58.9M^2 + 81.8T^2 + 147.9B^2 + 21.5GM + 13.3GT + 2.8GB - 24.3MT + 138.5MB - 50.0TB \quad (3)$$

where G, M, T, and B represent glucose, yeast extract, L-tyrosine, and $CuSO_4$ concentrations, respectively.

Regression analysis revealed that glucose had a positive effect on melanin production, whereas L-tyrosine exhibited a significant negative effect at higher concentrations. The positive contribution of glucose suggests its role as an efficient carbon source enhancing microbial metabolism and pigment synthesis, while excessive L-tyrosine concentrations may lead to substrate inhibition or metabolic imbalance. Although $CuSO_4$ showed a positive coefficient, its effect was not statistically significant, indicating a secondary role in melanin production. Similarly, yeast extract contributed positively but was not a significant factor. Interaction analysis demonstrates that the combination of high glucose and low L-tyrosine concentrations results in maximum melanin yield. Contour and surface plots (Figure 12) confirm that melanin production is maximized in regions characterized by low L-tyrosine and high glucose concentrations.

These findings are consistent with previous studies reporting glucose as an effective carbon source for melanin production and yeast extract as a supplier of essential nutrients that support microbial growth and enzymatic activity. L-tyrosine functions as a key precursor in melanin biosynthesis; however, excessive concentrations may inhibit production due to metabolic limitations. $CuSO_4$ acts as a cofactor for tyrosinase, a copper-dependent enzyme involved in melanin synthesis, and its optimal concentration is crucial for efficient pigment formation. Similar observations have been reported in previous

https://doi.org/10.1021/acsomega.6c03470
ACS Omega XXXX, XXX, XXX−XXX

Downloaded from pubs.acs.org/acsodf/article-pdf/doi/10.1021/acsomega.6c03470/6922768l/acsomega.6c03470.pdf by ANADOLU UNIV. Pervin Soyer on 18 November 2026

optimization studies, where balanced medium composition was essential for maximizing melanin yield. The results indicate that melanin production is strongly influenced by carbon source availability and precursor concentration. The optimized conditions identified in this study provide an effective strategy for enhancing melanin yield and demonstrate that microbial melanin production is a sensitive process governed by both nutritional and physicochemical parameters.

4. CONCLUSION

Melanin is a multifunctional natural pigment with considerable potential for applications in pharmaceutical, cosmetic, food, and biotechnological fields owing to its diverse physicochemical and biological properties. In this study, a halotolerant *Bacillus atrophaeus* isolate obtained from the hypersaline environment of Tuz Lake was identified as a novel microbial producer of melanin, and pigment production was successfully optimized using a Box−Behnken experimental design, resulting in a maximum yield of 1.773 g/L under the optimized culture conditions. Comprehensive physicochemical characterization demonstrated that the extracted pigment shared major structural and physicochemical features with commercial synthetic melanin. The combined UV−vis, FT-IR, DSC, SEM−EDS, ^{1}H NMR, and biosynthetic inhibition analyses consistently supported the classification of the extracted material as a predominantly DOPA-dependent eumelanin-like pigment. Nevertheless, because SEM−EDS provides only elemental information and detected a low sulfur content (1.37 wt %), while no nitrogen signal was observed owing to the limited sensitivity of EDS toward light elements, the precise molecular composition of the pigment cannot be established conclusively. Accordingly, the presence of a minor sulfur-containing melanin fraction or a heterogeneous eumelanin−pheomelanin-like composition cannot be completely excluded based on the currently available evidence. Biological evaluation demonstrated that the microbial pigment possesses promising antimicrobial, antioxidant, UV-protective, and biocompatible properties, highlighting its potential as a functional natural biomaterial. Compared with conventional melanin sources, microbial production offers important advantages, including sustainability, scalability, shorter production time, and reduced dependence on animal- or chemically derived pigments. Furthermore, the adaptation of the producing strain to the extreme hypersaline conditions of Tuz Lake may contribute to the distinctive physicochemical and biological characteristics of the obtained pigment, emphasizing hypersaline environments as valuable reservoirs for discovering functionally diverse microbial melanins. This study provides one of the most comprehensive investigations of melanin produced by a halotolerant *Bacillus atrophaeus* isolate by integrating production optimization, biosynthetic pathway analysis, structural characterization, and biological activity evaluation. These findings expand current knowledge of halotolerant microbial melanins and support their potential use as sustainable functional biomaterials for future pharmaceutical, cosmetic, and industrial applications. Future studies employing complementary high-resolution structural techniques, including electron paramagnetic resonance (EPR), X-ray photoelectron spectroscopy (XPS), solid-state NMR, targeted chemical degradation, and CHNS elemental analysis, together with pilot-scale production studies, will further elucidate the molecular architecture of the pigment and facilitate its industrial translation.

AUTHOR INFORMATION

Corresponding Author

Pervin Soyer − *Faculty of Pharmacy, Department of Pharmaceutical Microbiology, Anadolu University, 26470 Eskisehir, Turkiye;* orcid.org/0000-0002-6258-1993; Phone: +90(531)9499084; Email: pervinsoyer@anadolu.edu.tr

Authors

Semra İlhan − *Faculty of Science, Department of Biology, Eskişehir Osmangazi University, 26040 Eskisehir, Turkiye*

A. Alper Öztürk − *Faculty of Pharmacy, Department of Pharmaceutical Technology, Anadolu University, 26470 Eskisehir, Turkiye;* orcid.org/0000-0001-9596-0538

Yağmur Tunali − *Faculty of Pharmacy, Department of Pharmaceutical Microbiology, Anadolu University, 26470 Eskisehir, Turkiye*

Complete contact information is available at: https://pubs.acs.org/10.1021/acsomega.6c03470

Author Contributions

Pervin Soyer (PS): Conceptualization, Methodology, Experimental design, Investigation, Data curation, Formal analysis, Visualization, Writing—original draft, Writing—review and editing, Supervision, Project administration. Semra Ilhan (SI): Methodology, Resources, Validation, Supervision, Writing—review and editing. A. Alper Öztürk (AAÖ): DSC analysis, thermal characterization, interpretation of DSC data, and writing—review and editing. Yağmur Tunalı (YT): Investigation, Data curation, Visualization, Validation.

Funding

This work was financially supported by the Anadolu University Scientific Research Projects Commission under Rapid Support Project No. 3744.

Notes

The authors declare no competing financial interest.

ACKNOWLEDGMENTS

This work was supported by the Anadolu University Scientific Research Projects Coordination Unit under Rapid Support Project No. 3744. The authors gratefully acknowledge Anadolu University, Faculty of Pharmacy, for providing the necessary research infrastructure and laboratory facilities. The authors would like to express their sincere appreciation to Zerrin Cantürk for her valuable scientific guidance and insightful contributions. The authors also thank İremnur Özkan (M.Sc.) for her technical support and assistance throughout the study.

REFERENCES

(1) de Menezes, G. C. A.; de Medeiros, T. D. M.; de Oliveira Lima, I. G.; da Silva, M. B.; de Queiroz, A. C.; Duarte, A. W. F.; de Oliveira, V. M.; Rosa, L. H.; Bicas, J. L. Pigments Produced by Fungi and Bacteria from Extreme Environments. *Microbes in the Food Industry* 2023, pp 393−440.; CTYPE:STRING:BOOK.

(2) D'Ischia, M.; Wakamatsu, K.; Napolitano, A.; Briganti, S.; Garcia-Borron, J. C.; Kovacs, D.; Meredith, P.; Pezzella, A.; Picardo, M.; Sarna, T.; Simon, J. D.; Ito, S. Melanins and Melanogenesis: Methods, Standards, Protocols. *Pigment Cell Melanoma Res.* **2013**, *26* (5), 616−633.

(3) Solano, F. Melanins: Skin Pigments and Much More—Types, Structural Models, Biological Functions, and Formation Routes. *New J. Sci.* **2014**, *2014* (1), 1−28.

Downloaded from pubs.acs.org/acsodf/article-pdf/doi/10.1021/acsomega.6c03470/6922768l/acsomega.6c03470.pdf by ANADOLU UNIV. Pervin Soyer on 18 November 2026

(4) Dadachova, E.; Bryan, R. A.; Huang, X.; Moadel, T.; Schweitzer, A. D.; Aisen, P.; Nosanchuk, J. D.; Casadevall, A. Ionizing Radiation Changes the Electronic Properties of Melanin and Enhances the Growth of Melanized Fungi. *PLoS One* **2007**, *2* (5), No. e457.
(5) El-Naggar, N. E. A.; El-Ewasy, S. M. Bioproduction, Characterization, Anticancer and Antioxidant Activities of Extracellular Melanin Pigment Produced by Newly Isolated Microbial Cell Factories Streptomyces Glaucescens NEAE-H. *Sci. Rep.* **2017**, *7* (1), 42129.
(6) Sun, S.; Zhang, X.; Sun, S.; Zhang, L.; Shan, S.; Zhu, H. Production of Natural Melanin by Auricularia Auricula and Study on Its Molecular Structure. *Food Chem.* **2016**, *190*, 801−807.
(7) Pavan, M. E.; López, N. I.; Pettinari, M. J. Correction to: Melanin Biosynthesis in Bacteria, Regulation and Production Perspectives. *Appl. Microbiol. Biotechnol.* **2020**, *104* (4), 1821−1822.
(8) Pralea, I. E.; Moldovan, R. C.; Petrache, A. M.; Ilieş, M.; Hegheş, S. C.; Ielciu, I.; Nicoară, R.; Moldovan, M.; Ene, M.; Radu, M.; Uifălean, A.; Iuga, C. A. From Extraction to Advanced Analytical Methods: The Challenges of Melanin Analysis. *Int. J. Mol. Sci.* **2019**, *20* (16), 3943.
(9) Prota, G. Melanins, Melanogenesis and Melanocytes: Looking at Their Functional Significance from the Chemist's Viewpoint. *Pigment Cell Res.* **2000**, *13* (4), 283−293.
(10) Nakamura, L. K. Taxonomic Relationship of Black-Pigmented Bacillus Subtilis Strains and a Proposal for Bacillus Atrophaeus Sp. Nov. *Int. J. Syst. Bacteriol.* **1989**, *39* (3), 295−300.
(11) Gölü, T.; 'nde, A.; Katyon, B.; Değerlerinin Belirlenmesi, A.; Üniversitesi, A.; Fakültesi, Z.; Ürünleri, S.; Bölümü, M. Tuz Gölü (Aksaray)'nde Bazı Katyon ve Anyon Değerlerinin Belirlenmesi. *Ziraat Mühendisliği* **2020**, *0* (370), 104−114.
(12) Jigna, C.; Mira Gordhanbhai, P.; Kurian, K. N. Bacterial Melanin with Immense Cosmetic Potential Produced by Marine Bacteria < em > Bacillus Pumilus</Em> MIN3. *Preprints* **2022**.
(13) Ammanagi, A. I.; Shivasharana, C. T.; Krishnaveni, R.; Badiger, A. S.; Ramaraj, V. K.; Srinath, B. S.; Karthik, Y. A Biotechnological Approach to Optimization and Production of Melanin by Brevibacillus Invocatus Strain IBA, under Submerged Fermentation. *Biomedicine* **2022**, *42* (2), 318−324.
(14) Elsayis, A.; Hassan, S. W. M.; Ghanem, K. M.; Khairy, H. Suggested Sustainable Medical and Environmental Uses of Melanin Pigment From Halotolerant Black Yeast Hortaea Werneckii AS1. *Front. Microbiol.* **2022**, *13*, 871394.
(15) Pathan, A. N.; Pethe, A. S. Studies of Melanin Producing Bacteria and Extraction of Bacterial Melanin from Sewage Water. *Int. J. Appl. Res.* **2016**, *2* (6), 413−415.
(16) Raman, N. M.; Ramasamy, S. Genetic Validation and Spectroscopic Detailing of DHN-Melanin Extracted from an Environmental Fungus. *Biochem. Biophys. Rep.* **2017**, *12*, 98−107.
(17) Öztürk, A. A.; Namlı, İ.; Güleç, K.; Görgülü, Ş. Design of Lamivudine Loaded Nanoparticles for Oral Application by Nano Spray Drying Method: A New Approach to Use an Antiretroviral Drug for Lung Cancer Treatment. *Comb. Chem. High Throughput Screen.* **2020**, *23* (10), 1064−1079.
(18) Öztürk, A. A.; Başaran, E.; Şenel, B.; Demirel, M.; Sarıca, Ş. Synthesis, Characterization, Antioxidant Activity of Quercetin, Rutin and Quercetin-Rutin Incorporated β-Cyclodextrin Inclusion Complexes and Determination of Their Activity in NIH-3T3, MDA-MB-231 and A549 Cell Lines. *J. Mol. Struct.* **2023**, *1282*, 135169.
(19) Şahin, Ş.; Kaya-Tilki, E.; Baysal, M.; Öztürk, A. A. Preparation and Evaluation of Temozolomide Loaded PLGA Nanoparticles for the Treatment of Glioblastoma Multiforme. *Sci. Rep.* **2025**, *15* (1), 36194.
(20) Ghadge, V.; Kumar, P.; Singh, S.; Mathew, D. E.; Bhattacharya, S.; Nimse, S. B.; Shinde, P. B. Natural Melanin Produced by the Endophytic Bacillus Subtilis 4NP-BL Associated with the Halophyte Salicornia Brachiata. *J. Agric. Food Chem.* **2020**, *68* (25), 6854−6863.
(21) Solak, B.; Soyer, P.; Kaya-Tilki, E.; Öztürk, A. A. Evaluation of Antimicrobial Properties and Antioxidant Activity of Rosmarinic Acid Loaded Resomer RG 502 H Based Nanoparticles against Tert-Butyl Hydroperoxide-Induced Oxidative Stress: A Detailed Formulation, Characterization and Efficacy Determination. *J. Drug Delivery Sci. Technol.* **2025**, *106*, 106721.
(22) Karakaya, A.; Bağcı, E. R.; Soyer, P.; Daoud, N. E. H.; Erçetin, T.; Acar Çevik, U. Synthesis, In Vitro Antimicrobial, and Antioxidant Activities of Novel Thiazole Derivatives. *Chem. Biodivers.* **2026**, *23* (1), No. e03308.
(23) Öztürk, A. A.; Aygül, A.; Şenel, B. Influence of Glyceryl Behenate, Tripalmitin and Stearic Acid on the Properties of Clarithromycin Incorporated Solid Lipid Nanoparticles (SLNs): Formulation, Characterization, Antibacterial Activity and Cytotoxicity. *J. Drug Delivery Sci. Technol.* **2019**, *54* (11), 101240.
(24) Jabrayıl, S. M.; İsmayılova Rajab, N.; Jahangirova Rafik, İ.; Jafarova Bayram, S.; Alper Öztürk, A. Phyto-Functionalized Niosomal Gel for Acne Therapy: Dual Delivery of Clindamycin and Botanical Actives via a Sustained Topical Platform - in Vitro, Ex Vivo, in Silico and in Vivo Evaluation. *J. Drug Delivery Sci. Technol.* **2026**, *121*, 108313.
(25) Blois, M. S.; Blois, S. M.; Blois, S. M. Antioxidant Determinations by the Use of a Stable Free Radical. *Nature* **1958**, *181* (4617), 1199−1200.
(26) Choi, M. J.; Kim, Y. R. Antioxidant and Melanin-Reduction Effect of Mixed Extracts of Bixa Orellana, Ammi Majus, and Glycyrrhiza Glabra. *Microbiol. Biotechnol. Lett.* **2024**, *52* (1), 55−64.
(27) Xue, J.; Wang, Y.; Qi, X.; Zeng, W.; Zhang, Y.; Lei, H. The Physicochemical Properties and Antioxidant and Bacteriostatic Activities of Auricularia Auricula Melanin Modificated by Arginine. *J. Food Meas. Charact.* **2024**, *18* (9), 7443−7454.
(28) van Meerloo, J.; Kaspers, G. J. L.; Cloos, J. Cell Sensitivity Assays: The MTT Assay. *Methods Mol. Biol.* **2011**, *731*, 237−245.
(29) Mosmann, T. Rapid Colorimetric Assay for Cellular Growth and Survival: Application to Proliferation and Cytotoxicity Assays. *J. Immunol. Methods* **1983**, *65* (1−2), 55−63.
(30) Kaya-Tilki, E.; Öztürk, A. A.; Engür-Öztürk, S.; Dikmen, M. Enhanced Anti-Angiogenic Effects of Aprepitant-Loaded Nanoparticles in Human Umbilical Vein Endothelial Cells. *Sci. Rep.* **2024**, *14* (1), 19837.
(31) Çevikelli, T.; Güven Bölgen, U. M.; Öztürk, A. A.; Kandır, S.; Balcı Özyurt, A.; Akyüz-Çetin, S.; Çelenk, A.; Eroğlu Özkan, E.; Demirci Kayıran, S. Lavandula Angustifolia and Pinus Brutia Loaded Nanoemulsion Enhances In Vivo Burn Wound Healing: Histopathological and Cytokine-Based Mechanistic Evidence. *J. Drug Delivery Sci. Technol.* **2026**, *122*, 108372.
(32) Altıntop, M. D.; Çiftçi, K.; Şentürk, M. K.; Öztürk, A. A.; Altınpulluk, H.; Ertorun, İ.; Akalın Çiftçi, G. Development of a New Series of Thiazoles as EGFR-Targeted Anticancer Agents for NSCLC Therapy through Nanotechnological and Computer-Aided Approaches. *Bioorg. Chem.* **2026**, *178*, 109938.
(33) Li, C.; Ji, C.; Tang, B. Purification, Characterisation and Biological Activity of Melanin from Streptomyces Sp. *FEMS Microbiol. Lett.* **2018**, *365* (19), 1−8.
(34) Ye, M.; Guo, G. Y.; Lu, Y.; Song, S.; Wang, H. Y.; Yang, L. Purification, Structure and Anti-Radiation Activity of Melanin from Lachnum YM404. *Int. J. Biol. Macromol.* **2014**, *63*, 170−176.
(35) Suwannarach, N.; Kumla, J.; Watanabe, B.; Matsui, K.; Lumyong, S. Characterization of Melanin and Optimal Conditions for Pigment Production by an Endophytic Fungus, Spissiomyces Endophytica SDBR-CMU319. *PLoS One* **2019**, *14* (9), No. e0222187.
(36) Sella, S. R. B. R.; Vandenberghe, L. P. S.; Soccol, C. R. Bacillus Atrophaeus: Main Characteristics and Biotechnological Applications - a Review. *Crit. Rev. Biotechnol.* **2015**, *35* (4), 533−545.
(37) Stein, T.; Düsterhus, S.; Stroh, A.; Entian, K. D. Subtilosin Production by Two Bacillus Subtilis Subspecies and Variance of the Sbo-Alb Cluster. *Appl. Environ. Microbiol.* **2004**, *70* (4), 2349−2353.
(38) Oliveira-Nascimento, L.; Caricati, A. T. P.; Abdulack-Lopes, F.; Neves, L. C. M.; Caricati, C. P.; Penna, T. C. V.; Stephano, M. A. Bacillus Atrophaeus Inactivated Spores as a Potential Adjuvant for Veterinary Rabies Vaccine. *Vaccine* **2012**, *30* (23), 3351−3354.

Downloaded from pubs.acs.org/acsodf/article-pdf/doi/10.1021/acsomega.6c03470/6922768l/acsomega.6c03470.pdf by ANADOLU UNIV. Pervin Soyer on 18 November 2026

https://doi.org/10.1021/acsomega.6c03470
ACS Omega XXXX, XXX, XXX−XXX

(39) Carr, E. C.; Barton, Q.; Grambo, S.; Sullivan, M.; Renfro, C. M.; Kuo, A.; Pangilinan, J.; Lipzen, A.; Keymanesh, K.; Savage, E.; Barry, K.; Grigoriev, I. V.; Riekhof, W. R.; Harris, S. D. Deciphering the Potential Niche of Two Novel Black Yeast Fungi from a Biological Soil Crust Based on Their Genomes, Phenotypes, and Melanin Regulation. *bioRxiv* **2022**, 2021.12.03.471027.
(40) Iqbal, S.; Ismail, F. Identification of Fungal Melanin Production and the Role of Anti-Melanin Agents. *Pak. J. Pharm. Sci.* **2023**, *36* (5), 1483−1488.
(41) Zhan, F.; He, Y.; Zu, Y.; Li, T.; Zhao, Z. Characterization of Melanin Isolated from a Dark Septate Endophyte (DSE), Exophiala Pisciphila. *World J. Microbiol. Biotechnol.* **2011**, *27* (10), 2483−2489.
(42) Aghajanyan, A. E.; Hambardzumyan, A. A.; Minasyan, E. V.; Tsaturyan, A. H.; Paloyan, A. M.; Avetisyan, S. V.; Hovsepyan, A. S.; Saghyan, A. S. Development of the Technology for Producing Water-Soluble Melanin from Waste of Vinary Production and the Study of Its Physicochemical Properties. *Eur. Food Res. Technol.* **2022**, *248* (2), 485−495.
(43) Wakamatsu, K.; Ito, S. Advanced Chemical Methods in Melanin Determination. *Pigment Cell Res.* **2002**, *15* (3), 174−183.
(44) Abbas, M.; D'Amico, F.; Morresi, L.; Pinto, N.; Ficcadenti, M.; Natali, R.; Ottaviano, L.; Passacantando, M.; Cuccioloni, M.; Angeletti, M.; Gunnella, R. Structural, Electrical, Electronic and Optical Properties of Melanin Films. *Eur. Phys. J. E Soft Matter* **2009**, *28* (3), 285−291.
(45) Wolbarsht, M. L.; Walsh, A. W.; George, G. Melanin, a Unique Biological Absorber. *Appl. Opt.* **1981**, *20* (13), 2184−2186.
(46) Palani, P.; Shree, C. G. Microbial Production and Characterization of 3, 4-Dihydroxy-L Phenylalanine Mediated an Extracellular Heterogenic Eumelanin Pigment From Marine Actinomycetes Prauserella Sp. MAPPL 017A. *Preprint* **2026**.
(47) Hou, R.; Liu, X.; Xiang, K.; Chen, L.; Wu, X.; Lin, W.; Zheng, M.; Fu, J. Characterization of the Physicochemical Properties and Extraction Optimization of Natural Melanin from Inonotus Hispidus Mushroom. *Food Chem.* **2019**, *277*, 533−542.
(48) Bell, A. A.; Wheeler, M. H. Biosynthesis and Functions of Fungal Melanins. *Annu. Rev. Phytopathol.* **1986**, *24* (1), 411−451.
(49) Liu, S.; Youngchim, S.; Zamith-Miranda, D.; Nosanchuk, J. D. Fungal Melanin and the Mammalian Immune System. *J. Fungi* **2021**, *7* (4), 264.
(50) Liu, Q.; Xiao, J.; Liu, B.; Zhuang, Y.; Sun, L. Study on the Preparation and Chemical Structure Characterization of Melanin from Boletus Griseus. *Int. J. Mol. Sci.* **2018**, *19* (12), 3736.
(51) Drewnowska, J. M.; Zambrzycka, M.; Kalska-Szostko, B.; Fiedoruk, K.; Swiecicka, I. Melanin-Like Pigment Synthesis by Soil Bacillus Weihenstephanensis Isolates from Northeastern Poland. *PLoS One* **2015**, *10* (4), No. e0125428.
(52) Öztürk, A. A.; Arpagaus, C. Nano Spray-Dried Drugs for Oral Administration: A Review. *Assay Drug Dev. Technol.* **2021**, *19* (7), 412−441.
(53) Öztürk, A. A.; Güven, U. M.; Yenilmez, E.; Şenel, B. Effects of Different Derivatives of Eudragit Polymer on Entrapment Efficiency, In Vitro Dissolution, Release Kinetics and Cell Viability Results on Extended Release Flurbiprofen Loaded Nanomedicines. *Lat. Am. J. Pharm.* **2018**, *37* (10), 1981−1992.
(54) Kiran, G. S.; Jackson, S. A.; Priyadharsini, S.; Dobson, A. D. W.; Selvin, J. Synthesis of Nm-PHB (Nanomelanin-Polyhydroxy Butyrate) Nanocomposite Film and Its Protective Effect against Biofilm-Forming Multi Drug Resistant Staphylococcus Aureus. *Sci. Rep.* **2017**, *7* (1), 9167.
(55) Kim, Y.; Park, H.; Lee, P.; Woo, K.; Choi, K.-Y.; Lee, H. H. Biosynthesis of Tyrosine-Derived i-Melanin and Its Characteristics for Organic Thin Film Transistor Device. *Mater. Today Adv.* **2025**, *26*, 100582.
(56) Gómez-Marín, A. M.; Sánchez, C. I. Thermal and Mass Spectroscopic Characterization of a Sulphur-Containing Bacterial Melanin from Bacillus Subtilis. *J. Non. Cryst. Solids* **2010**, *356* (31−32), 1576−1580.
(57) Elsayis, A.; Hassan, S. W. M.; Ghanem, K. M.; Khairy, H. Suggested Sustainable Medical and Environmental Uses of Melanin Pigment From Halotolerant Black Yeast Hortaea Werneckii AS1. *Front. Microbiol.* **2022**, *13*, 871394.
(58) Elsayis, A.; Hassan, S. W. M.; Ghanem, K. M.; Khairy, H. Optimization of Melanin Pigment Production from the Halotolerant Black Yeast Hortaea Werneckii AS1 Isolated from Solar Salter in Alexandria. *BMC Microbiol.* **2022**, *22* (1), 92.
(59) Gunde-Cimerman, N.; Ramos, J.; Plemenitaš, A. Halotolerant and Halophilic Fungi. *Mycol. Res.* **2009**, *113* (11), 1231−1241.
(60) Mbonyiryivuze, A.; Y. Nuru, Z.; Diop Ngom, B.; Mwakikunga, B.; Mokhotjwa Dhlamini, S.; Park, E.; Maaza, M. Morphological and Chemical Composition Characterization of Commercial Sepia Melanin. *Am. J. Nanomater.* **2015**, *3* (1), 22−27.
(61) Ferraz, A. R.; Pacheco, R.; Vaz, P. D.; Pintado, C. S.; Ascensão, L.; Serralheiro, M. L. Melanin: Production from Cheese Bacteria, Chemical Characterization, and Biological Activities. *Int. J. Environ. Res. Public Health* **2021**, *18* (20), 10562.
(62) Wu, C. C.; Li, H.; Yin, Z. W.; Zhang, H. T.; Gao, M. J.; Zhu, L.; Zhan, X. B. Isolation, Purification, and Characterization of Novel Melanin from the Submerged Fermentation of Rhizobium Radiobacter. *Process Biochem.* **2022**, *121*, 263−275.
(63) Wang, L. F.; Rhim, J. W. Isolation and Characterization of Melanin from Black Garlic and Sepia Ink. *LWT* **2019**, *99*, 17−23.
(64) Kumar, C. G.; Mongolla, P.; Pombala, S.; Kamle, A.; Joseph, J. Physicochemical Characterization and Antioxidant Activity of Melanin from a Novel Strain of Aspergillus Bridgeri ICTF-201. *Lett. Appl. Microbiol.* **2011**, *53* (3), 350−358.
(65) Mathew, D.; G Bhat, S. Pseudomonas Stutzeri as Biofactories for Melanin Nanoparticle Synthesis and Its Anti-Oxidative and Antibiofilm Potential Evaluation. *Bionanoscience* **2022**, *12* (3), 912.
(66) Tarangini, K.; Mishra, S. Production of Melanin by Soil Microbial Isolate on Fruit Waste Extract: Two Step Optimization of Key Parameters. *Biotechnol. Rep.* **2014**, *4* (1), 139−146.
(67) Öztürk, A. A.; Banderas, L. M.; Otero, M. D. C.; Yenilmez, E.; Şenel, B.; Yazan, Y. Dexketoprofen Trometamol-Loaded Poly-Lactic-Co-Glycolic Acid (PLGA) Nanoparticles: Preparation, in Vitro Characterization and Cyctotoxity. *Trop. J. Pharm. Res.* **2019**, *18* (1), 1−11.
(68) Boukamp, P.; Petrussevska, R. T.; Breitkreutz, D.; Hornung, J.; Markham, A.; Fusenig, N. E. Normal Keratinization in a Spontaneously Immortalized Aneuploid Human Keratinocyte Cell Line. *J. Cell Biol.* **1988**, *106* (3), 761−771.
(69) Oh, J. J.; Kim, J. Y.; Son, S. H.; Jung, W. J.; Kim, D. H.; Seo, J. W.; Kim, G. H. Fungal Melanin as a Biocompatible Broad-Spectrum Sunscreen with High Antioxidant Activity. *RSC Adv.* **2021**, *11* (32), 19682−19689.
(70) Rastogi, R. P.; Richa; Kumar, A.; Tyagi, M. B.; Sinha, R. P. Molecular Mechanisms of Ultraviolet Radiation-Induced DNA Damage and Repair. *J. Nucleic Acids* **2010**, *2010*, 592980.
(71) Moeller, R.; Horneck, G.; Facius, R.; Stackebrandt, E. Role of Pigmentation in Protecting Bacillus Sp. Endospores against Environmental UV Radiation. *FEMS Microbiol. Ecol.* **2005**, *51* (2), 231−236.
(72) Patki, J. M.; Singh, S.; Singh, S.; Padmadas, N.; Dasgupta, D. Analysis of the Applicative Potential of Pigments Extracted from Bacterial Isolates of Mangrove Soil as Topical UV Protectants. *Braz. J. Pharm. Sci.* **2021**, *57*, No. e19127.
(73) Pal, A. K.; Gajjar, D. U.; Vasavada, A. R. DOPA and DHN Pathway Orchestrate Melanin Synthesis in Aspergillus Species. *Med. Mycol.* **2013**, *52* (1), 1−9.
(74) Surwase, S. N.; Jadhav, S. B.; Phugare, S. S.; Jadhav, J. P. Optimization of Melanin Production by Brevundimonas Sp. SGJ Using Response Surface Methodology. *3 Biotech* **2013**, *3* (3), 187−194.

Downloaded from pubs.acs.org/acsodf/article-pdf/doi/10.1021/acsomega.6c03470/6922768l/acsomega.6c03470.pdf by ANADOLU UNIV. Pervin Soyer on 18 November 2026

https://doi.org/10.1021/acsomega.6c03470
ACS Omega XXXX, XXX, XXX−XXX